



Review

The Impact of Adsorption Property Modification by Crosslinkers on Graphene Oxide Membrane Separation Performance

Martin Ayala-Claveria ¹, Carlos Carlesi ^{1,*} , Julieta Puig ²  and Gianni Olguin ¹

¹ Escuela de Ingeniería Química, Facultad de Ingeniería, Pontificia Universidad Católica de Valparaíso, Avenida Brasil 2162, Valparaíso 2362854, Chile; martin.ayala@pucv.cl (M.A.-C.); gianni.olguin@pucv.cl (G.O.)

² Instituto de Investigaciones en Ciencia y Tecnología de Materiales (INTEMA), Consejo Nacional de Investigaciones Científicas y Técnicas/Universidad Nacional de Mar del Plata (CONICET/UNMdP), Av. Colón 10850, Mar del Plata B7606WV, Argentina; julietapuig@fi.mdp.edu.ar

* Correspondence: carlos.carlesi@pucv.cl

Abstract: The health risks associated with the presence of heavy metals in drinking water can be severe. To address this issue, membrane separation technology is one of the consolidated alternatives. Inorganic, porous membranes were found in applications where low energy consumption is highly desirable. The selectivity of these membranes is attained by functionalisation. Graphene oxide functionalised membrane technology is promising for removing heavy metal ions. This work summarises, discusses and presents the relationship between adsorption and overall membrane separation process performance for heavy metal ions removal from wastewater when a graphene oxide-functionalised membrane is used. The separation performance depends on the hydrophobic interactions of the membrane and the solute. The electrostatic interaction between the negatively charged membrane surface and positively charged metal ions facilitates the adsorption, leading to the rejection of these metal ions. The influences of the chemical nature of the modifiers of graphene oxide layers are highlighted.

Keywords: heavy metal pollution; graphene oxide membrane; metal adsorption; graphene oxide crosslinker; covalent linker



Citation: Ayala-Claveria, M.; Carlesi, C.; Puig, J.; Olguin, G. The Impact of Adsorption Property Modification by Crosslinkers on Graphene Oxide Membrane Separation Performance. *Processes* **2024**, *12*, 2320. <https://doi.org/10.3390/pr12112320>

Academic Editor: Piotr Rybarczyk

Received: 17 September 2024

Revised: 18 October 2024

Accepted: 21 October 2024

Published: 23 October 2024



Copyright: © 2024 by the authors. Licensee MDPI, Basel, Switzerland. This article is an open access article distributed under the terms and conditions of the Creative Commons Attribution (CC BY) license (<https://creativecommons.org/licenses/by/4.0/>).

1. Introduction

The presence of heavy metals in drinking water can cause severe hazards to human health. Although they are naturally occurring elements, their multiple uses in industry, household, agriculture and medicine have contributed to their concentration in the environment close to industrial activity, thus increasing the recognition of their potentially harmful effects on human life and the environment [1]. For example, exposure to elevated levels of metallic, organic and inorganic mercury can damage the brain, kidneys and the developing foetus [2]. Various technologies, including precipitation–coagulation–flocculation, adsorption, ion exchange, flotation and membrane-based separation, have been developed to remove heavy metal ions (HMI) from wastewater [3–5]. The process of precipitation, coagulation–flocculation and ion exchange work efficiently when pollutant concentration is medium to high (over 100 ppm), thus requiring further removal techniques to attain the restrictive level needed in the case of heavy metals pollution. Alternatives for this last removal step are adsorption- [6] and membrane-based [7] separation processes.

Nowadays, membrane process reverse osmosis (RO) is the dominant technique in large-scale water treatment and is also applied to heavy metal removal [8–11]. The results showed that RO could achieve up to 99% removal efficiency of Cu²⁺, Ni²⁺, Zn²⁺ and As⁵⁺. However, the main limitation of RO application is the high power consumption and operating cost [12,13] due to high pressures (15–75 bar). This drawback relies on the low water permeability of RO membranes, showing fluxes around 2–5 L m⁻² h⁻¹ bar⁻¹ [14]. On the other hand, the high permeability and selectivity of ceramic membranes could

allow higher water flux ($8\text{--}40\text{ L m}^{-2}\text{ h}^{-1}\text{ bar}^{-1}$ [15]) and show high recovery and improved energy savings [16]. However, overcoming challenges such as reducing the capital cost [17], long-term stability [18] and scalability [19] would enable ceramic membranes to consolidate in the water treatment market. Graphene oxide (GO) stands out for its numerous properties among ceramic materials. For this reason, a wide range of applications have been explored, aiming at commercialisation [20] and offering significant environmental and economic benefits [21]. The main problem with GO membranes is the loss of stability over long periods of operation [22].

The long-term stability of GO membranes is mainly triggered by water molecules connecting with oxygenated groups located elsewhere in the GO structure, thus promoting the widening of nanochannels and allowing the transport of pollutant ions. This instability can be overcome by incorporating covalent or non-covalent binding additives within the GO matrix [23], commonly known as crosslinkers. Nevertheless, adding a new component to the GO alters the chemical nature of the matrix, and it could be responsible for a new behaviour towards rejecting specific contaminants.

Adsorption is the process taking place when a solute (adsorbate) accumulates on the surface of a solid (adsorbent) and forms a molecular or atomic film [6], while membrane-based separation is the process of using a barrier that inhibits the passage of certain constituents while allowing other constituents to pass through [24]. These techniques are commonly described as separate alternatives, but could they be related in their mechanisms of operation?

In the literature, several works refer to the adsorption or nanofiltration of heavy metal ions. However, none of the studies focus on the influence adsorption could have on the performance of membrane-based processes for wastewater treatment. For example, Burakov et al. [6] present a detailed review of the adsorption of noxious heavy metal ions from wastewater effluents using various adsorbents, such as conventional and nanostructured. Xiang et al. [25] review the latest developments, discoveries and prospective applications related to ultrafiltration, nanofiltration, reverse osmosis and electrodialysis, with an in-depth focus on heavy metal removal. Abadi et al. [26] have summarised and analysed processes in which nanofibers prepared by the electrospinning method were used as a photocatalyst or adsorbent in wastewater treatment.

The present work aims to describe the connection between adsorption and membrane-based processes, analysing experimental results for HMI removal from water when using functionalised graphene oxide inorganic membranes and the effect of the modification of the material with crosslinkers and covalent linkers between GO layers.

The review focuses on the relationship between adsorption and selectivity of GO membranes and considers only the data available referring to membrane performance, not including particular data for adsorption studies outside the context of membrane separation processes.

2. Adsorption of Heavy Metal Ions on Graphene Oxide

Graphene oxide (GO) is a compound derived from graphene, a single layer of carbon atoms arranged in a two-dimensional honeycomb lattice oxide. It usually contains hydroxyl, carboxyl, and epoxide functional groups on its surface. In combination with its high surface area, the material has a high adsorption capacity for the removal of HMI from aqueous solutions [27].

Table 1 shows the maximum adsorption capacity (q_{max}), which represents an adsorbent's overall adsorption capability [28]. GO has a strong adsorption affinity to various heavy metal ions, and the maximum adsorption capacities are generally more significant than those of other adsorbents [5,6]. For example, Šljivić et al. [29] demonstrated that Cu(II) adsorption in zeolite was 8.13 mg g^{-1} (pH 5.0, T 298 K), while in GO, it is 294.00 mg g^{-1} [30] at the same conditions. Khosravi et al. [31] determined that amino-functionalized zeolite imidazolate framework-8 (ZIF-8-EDA) possesses a maximum adsorption capacity of Cd(II), equivalent to half the maximum adsorption capacity of GO. This can be explained by the

negative charge on the surface of GO nanosheets in aqueous solutions due to the ionisation of the carboxylic groups and the lone-pair oxygen atoms in GO. Consequently, GO is an ideal sorbent to bind metal ions through ionic and coordinative interaction [32]. Also, the complexation of heavy metal species with surface oxygenous functional groups (e.g., $-\text{OH}$ and $-\text{COOH}$) is also one possible adsorption mode [33].

Table 1. Maximum adsorption capacities of heavy metal ions using different sorbents.

Adsorbed Heavy Metal Ions	Type of Sorbent	q_{max} (mg g ⁻¹)	Operating Conditions	Adsorption Isotherm Models	Reference
As(III)	GO	1432.80	pH N.A., T N.A.	Langmuir	[34]
		0.02	pH 7, T 298 K	Langmuir	[35]
Au(III)	GO	149.20	pH N.A., T 298 K	Langmuir	[36]
Cd(II)	GO	83.80	pH 5.7, T 305 K	Langmuir	[37]
		530.00	pH 5.0, T 298 K	Langmuir	[30]
Co(II)	Ze-nWRT	270.00	pH 4.0, T 307 K	Langmuir	[38]
	ZIF-8-EDA	294.11	pH 6.0, T N.A.	Langmuir	[31]
	GO	21.28	pH 5.5, T 298 K	Freundlich	[39]
	LL-NaOH	25.40	pH 6.0, T 301 K	Langmuir	[40]
Cr(VI)	GO	1.22	pH 4.0, T N.A.	Langmuir	[41]
Cu(II)	GO	46.60	pH 5.0, T N.A.	Langmuir	[42]
		72.60	pH 5.7, T 303 K	Langmuir	[37]
		294.00	pH 5.0, T 298 K	Langmuir	[30]
	LC-Al ₂ O ₃	117.50	pH 5.3, T N.A.	Freundlich	[43]
		15.69	pH 5.0, T 298 K	Langmuir	[44]
		23.18	pH 5.0, T 298 K	Langmuir	[45]
Eu(III)	GO	175.44	pH 6.0, T 298 K	Langmuir	[46]
	TNRs	115.30	pH 5.0, T N.A.	Langmuir	[47]
Hg(II)	GO	8.65	pH N.A., T 298 K	Intraparticle diffusion	[48]
Mn(II)	GO	32.00	pH 5.0, T 298 K	Langmuir	[49]
Ni(II)	GO	62.30	pH 5.7, T 304 K	Langmuir	[37]
		38.61	pH 6.0, T 298 K	Langmuir	[50]
		250.00	pH 6.0, T 298 K	N.A.	[51]
Pb(II)	GO	842.00	pH 6.0, T 293 K	Langmuir	[52]
		1119.00	pH 5.0, T 298 K	Langmuir	[30]
Sb(III)	GO	8.06	pH 11.0, T 303 K	Freundlich	[53]
Sr(II)	GO	5.93	pH 3.0, T 293 K	Langmuir	[54]
Th(IV)	GO	58.59	pH 1.4, T 293 K	Langmuir	[55]
U(VI)	GO	299.00	pH 4.0, T 298 K	Langmuir	[56]
		5.12	pH 3.0, T 293 K	Langmuir	[54]
Zn(II)	TNRs	282.50	pH 5.0, T N.A.	Langmuir	[47]
	GO	246.00	pH 7.0, T 293 K	Langmuir	[57]
		345.00	pH 5.0, T 298 K	Langmuir	[30]

q_{max} : maximum adsorption capacity; T: temperature of adsorption; N.A.: not available.

The adsorption capacity of a material is influenced by both pH and temperature. Table 1 presents the operating conditions for achieving maximum adsorption capacity. To increase the attraction between GO and HMI, the solution is brought to a pH above pH_{pzc} (point of zero charge), where the surface charge of GO is negative, and the electrostatic interactions become stronger [30]. Furthermore, Table 1 presents the adsorption isotherm models where the Langmuir model indicates that the adsorbent surface contains only a certain number of active sites for a single molecule to be adsorbed, while the Freundlich model indicates that there are several different adsorption sites on a heterogeneous adsorbent material. According to the data, metal ions fit the Langmuir model best, describing the chemisorption process when ionic or covalent chemical bonds are formed between the adsorbent (GO) and the adsorbate (HMI) [58].

3. Adsorption of Heavy Metal Ions on Modified Graphene Oxide

Different materials have been used to modify graphene oxide and improve its stability and capacity. These compounds, called crosslinkers, have different characteristic functional groups, which allow the structure and properties of the GO to be modified. The modification of GO with carboxylic acids [59], diamines [59–61], dialdehydes [62], metal groups [63,64], and amino acids [65] has been widely reported, where the functional group is the main responsible for the cross-linking to the GO layer through chemical bonds or physical interactions. Chemical functionalisation of GO nanosheets is usually carried out in temperature-assisted solution [66], layer-by-layer deposition [67,68], use of the sol-gel method [69] or immersion in solution with the crosslinker [70]. In addition to crosslinkers, GO can also be improved by adding a second compound, called a covalent linker, which increases the number of covalent bonds between the functionalised GO sheets and the contaminants. The incorporation of a covalent linker within the functionalised GO membrane structure can be performed directly into the synthesis GO-crosslinker solution or by immersing the already functionalised GO-crosslinker membrane in a solution containing the second functional material [70].

Table 2 shows the maximum adsorption capacities of most heavy metal ions on modified GO. It can be observed that the adsorption capacity is higher than those on unmodified GO (Table 1). This suggests that the materials used to modify GO enhance the adsorption capacity of the modified GO composites. Figure 1a depicts the box plots for the data presented in Tables 1 and 2, showing a clear difference between GO material with or without additives. The addition of a crosslinker into the GO matrix increases the adsorption of heavy metal ions, showing a median twofold superiority to unmodified GO. Crosslinkers may incorporate more connection sites between the material and the heavy metal ion; for example, nitrogen-based crosslinkers have one connection point per nitrogen atom, and oxygen-based crosslinkers have two connection points per oxygen atom. Metal crosslinkers have electrostatic interactions with metal ions. However, adding a second material seems to decrease the adsorption, likely due to the bonding between the covalent linker and the GO functionalised nanosheets (decreasing the connection sites for the metal ions). In the case of GO, the maximum adsorption capacity is $253.58 \pm 75.39 \text{ mg g}^{-1}$, while for GO-crosslinker and GO-crosslinker-covalent linker, the maximum capacity is $362.89 \pm 48.86 \text{ mg g}^{-1}$ and $128.41 \pm 26.15 \text{ mg g}^{-1}$.

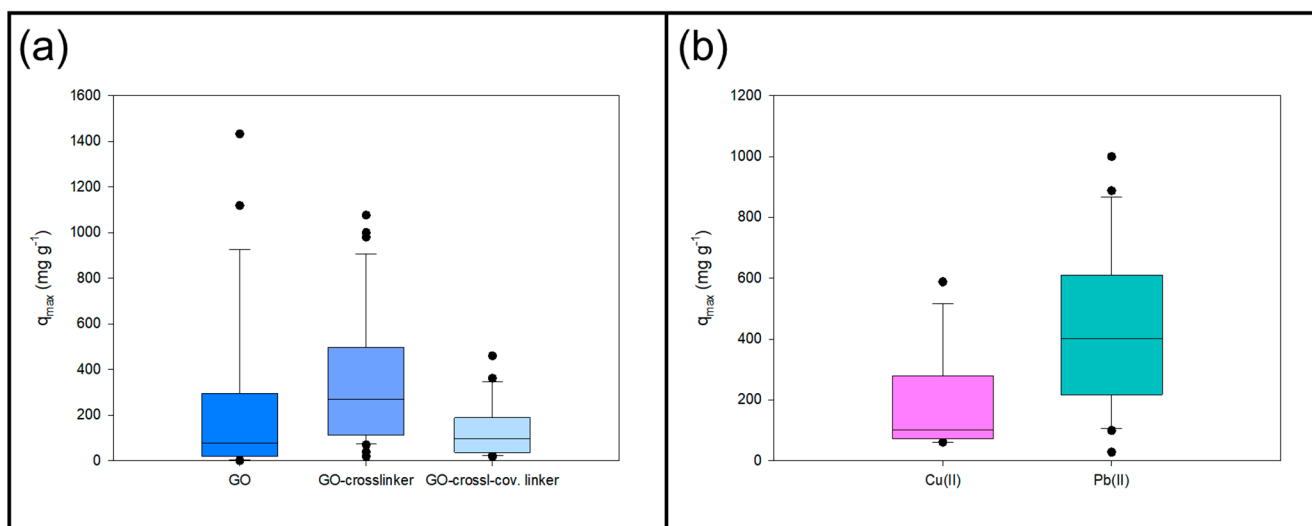


Figure 1. Box plot of (a) maximum adsorption capacities of GO and GO-based composites; (b) maximum adsorption capacities of Cu(II) and Pb(II) using GO-based composites.

Figure 1b depicts the box plot of the maximum adsorption of capacities for Cu(II) and Pb(II) using GO-based materials. It is noticeable that, despite having the same ionic charges,

the adsorption has different values. This is because the q_{max} is related to the characteristics of the metal ion, in addition to the properties of the GO-based sorbent [71].

In Table 2, both the crosslinker and covalent linker are classified in terms of the dominant functional groups and are denoted according to the connecting element between the compound and the GO nanosheet: nitrogen (N), oxygen (O) and metallic element (M).

Table 2. Maximum adsorption capacities of crosslinker and crosslinker-covalent linker-functionalised GO for removing heavy metal ions.

Heavy Metal Ion	Crosslinker (Classification)	Chemical Formula Crosslinker *	Covalent Linker (Classification)	Chemical Formula Covalent Linker *	q_{max} (mg g ⁻¹)	Operating Condition	Reference
As(V)	Fe-NPs (M)	Fe ₃ O ₄	-	-	73.42	pH 7.0, T 298 K	[72]
Au(III)	CS (N, O)	C ₆ H ₁₁ NO ₄	-	-	1076.65	pH 4.0, T 323 K	[36]
	PAM (N, O)	C ₃ H ₅ NO	-	-	253.81	pH 5.0, T 298 K	[73]
	PEI (N)	C ₂ H ₅ N	PDA (N)	C ₇ H ₉ NO ₂	106.00	pH 5.2–6.8	[74]
	Fe-NPs (M)	Fe ₃ O ₄	EDA (N)	C ₂ H ₈ N ₂	27.83	pH 6.0–7.0, T 293 K	[75]
	PDA (N)	C ₇ H ₉ NO ₂	-	-	210.00	T 298 K	[76]
	PDA (N)	C ₇ H ₉ NO ₂	-	-	-	pH 6.0	[77]
Co(II)	PPhDA (N)	C ₆ H ₈ N ₂	-	-	116.35	pH 6.0, T 298 K	[78]
Cr(VI)	MgAl-LDH (M)	-	-	-	172.55	pH 2.0, 293 K	[79]
	Fe-NPs (M)	Fe ₃ O ₄	CS (N, O)	C ₆ H ₁₁ NO ₄	162.00	pH 4.25, T 293 K	[80]
	TETA (N)	C ₆ H ₁₈ N ₄	-	-	219.50	pH 2.0, T 303 K	[81]
	PAAm (N)	C ₃ H ₇ N	-	-	485.00	pH 4.0, T 298 K	[82]
	Fe-NPs (M)	Fe ₃ O ₄	EDA (N)	C ₂ H ₈ N ₂	17.29	pH 1.0–3.0, T 293 K	[75]
	CDx (O)	C ₄₂ H ₇₀ O ₃₅	CS (N)	C ₆ H ₁₁ NO ₄	67.66	T 298 K	[83]
	Fe-NPs (M)	Fe ₃ O ₄	CS (N)	C ₆ H ₁₁ NO ₄	107.99	pH 2.0, T 303 K	[84]
	Fe-NPs (M)	Fe ₃ O ₄	DACHTA (N)	C ₁₄ H ₂₂ N ₂ O ₈	83.66	pH 3.0, T 303 K	[85]
Cu(II)	Fe-NPs (M)	Fe ₃ O ₄	SAC (O)	C ₆ H ₆ NO ₃ S	62.73	pH 5.0, T 298 K	[86]
	EDTA (N, O)	C ₁₀ H ₁₄ N ₂ O ₈	-	-	301.20	T 318 K	[87]
	Ca ²⁺ (M)	-	SA (O)	C ₆ H ₉ NaO ₇	60.20	-	[88]
	TETA (N)	C ₆ H ₁₈ N ₄	-	-	209.10	pH 6.0, T 293 K	[89]
	SA (O)	C ₆ H ₉ NaO ₇	-	-	98.00	pH 5.0, T 303 K	[90]
	PAM (N, O)	C ₃ H ₅ NO	-	-	68.68	pH 4.5, T 298 K	[73]
	PEI (N)	C ₂ H ₅ N	PDA (N)	C ₇ H ₉ NO ₂	87.00	pH 5.2–6.8	[74]
	PAAm (N)	C ₃ H ₇ N	-	-	349.04	pH 6.0, T 293 K	[91]
	L-Trp (N, O)	C ₁₀ H ₁₂ N ₂ O ₂	-	-	588.00	pH 5.0, T 293 K	[92]
	ATP (N, O)	C ₆ H ₇ NS	-	-	99.17	pH 6.0, T 298 K	[93]
	APTES (N, M)	C ₉ H ₂₃ NSiO ₃	-	-	103.28	pH 6.0, T 298 K	[93]
	EDTA (N, O)	C ₁₀ H ₁₄ N ₂ O ₈	-	-	108.70	pH 5.0	[94]
Hg(II)	EDTA (N, O)	C ₁₀ H ₁₄ N ₂ O ₈	-	-	268.40	T 318 K	[87]
	PPy (N)	C ₈ H ₆ N ₂	-	-	980.00	pH 3.0, T 293 K	[95]
	PEI (N)	C ₂ H ₅ N	PDA (N)	C ₇ H ₉ NO ₂	110.00	pH 3.5–4.0	[74]
	Co-NPs (M)	Co ₃ O ₄	CS (N, O)	C ₆ H ₁₁ NO ₄	361.00	pH 7.0, T 323 K	[96]
	Fe-NPs (M)	Fe ₃ O ₄	EDA (N)	C ₂ H ₈ N ₂	23.03	pH 6.0–7.0, T 293 K	[94]
Mn(II)	PAM (N, O)	C ₃ H ₅ NO	-	-	18.29	pH 4.0, T 298 K	[73]
Ni(II)	Gly (N, O)	C ₂ H ₅ NO ₂	-	-	36.63	pH 6.0, T 293 K	[50]
	Fe-NPs (M)	Fe ₃ O ₄	EDA (N)	C ₂ H ₈ N ₂	22.07	pH 6.0–7.0, T 293 K	[94]
Pb(II)	EDTA (N, O)	C ₁₀ H ₁₄ N ₂ O ₈	-	-	508.40	T 318 K	[87]
	EDTA (N, O)	C ₁₀ H ₁₄ N ₂ O ₈	-	-	479.00	pH 6.8, T 298 K	[97]
	CS (N, O)	C ₆ H ₁₁ NO ₄	-	-	120.00	pH 6.0, T 298 K	[98]
	PAM (N, O)	C ₃ H ₅ NO	-	-	1000.00	pH 6.0, T 298 K	[99]
	CS (N, O)	C ₆ H ₁₁ NO ₄	-	-	99.00	T Room	[100]
	PVK (N)	C ₁₄ H ₁₁ N	-	-	887.98	pH 7.0, T 298 K	[101]
	APTES (N, O, M)	C ₉ H ₂₃ NSiO ₃	-	-	312.50	pH 4–5, T 303 K	[102]
	PAM (N, O)	C ₃ H ₅ NO	-	-	819.67	pH 6.0, T 293 K	[103]
	SA (O)	C ₆ H ₉ NaO ₇	-	-	267.40	pH 5.5, T 303 K	[90]
	CS (N, O)	C ₆ H ₁₁ NO ₄	-	-	216.92	pH 3.0, T 323 K	[36]
	PAAM (N, O)	C ₃ H ₅ NO	-	-	568.18	pH 4.5, T 298 K	[73]
	LS (O)	C ₂₀ H ₂₄ Na ₂ O ₁₀ S ₂	PANI (N)	C ₆ H ₅ N	216.40	pH 5.0, T 303 K	[104]
	PEI (N)	C ₂ H ₅ N	PDA (N)	C ₇ H ₉ NO ₂	197.00	pH 4.0–5.4	[74]
	OphDA (N)	C ₆ H ₈ N ₂	PDA (N)	C ₇ H ₉ NO ₂	228.0	-	[105]
	PAM (N, O)	C ₃ H ₅ NO	-	-	819.67	pH 6.0, T 293 K	[103]

Table 2. Cont.

Heavy Metal Ion	Crosslinker (Classification)	Chemical Formula Crosslinker *	Covalent Linker (Classification)	Chemical Formula Covalent Linker *	q_{max} (mg g ⁻¹)	Operating Condition	Reference
Sr(II) U(VI)	L-Trp (N, O)	C ₁₀ H ₁₂ N ₂ O ₂	-	-	222.00	pH 4.0, T 293 K	[92]
	Fe-NPs (M)	Fe ₃ O ₄	L-Cys	C ₃ H ₇ NO ₂ S	459.33	pH 6.0	[106]
	HPEI (N)	C ₂ H ₅ N	-	-	438.6	pH 5.5, T 298 K	[107]
	Fe-NPs (M)	Fe ₃ O ₄	EDA (N)	C ₂ H ₈ N ₂	27.95	pH 6.0–7.0, T 293 K	[94]
	PDA (N)	C ₇ H ₉ NO ₂	-	-	365.00	T 298 K	[76]
	HPA (N)	C ₅ H ₁₅ N ₃	-	-	740.7	pH 5.9, T 298 K	[108]
	PDA (N)	C ₇ H ₉ NO ₂	-	-	-	pH 6.0	[77]
	EDTA (N, O)	C ₁₀ H ₁₄ N ₂ O ₈	-	-	454.60	pH 3.0	[94]
	PAM (N, O)	C ₃ H ₅ NO	-	-	184.88	pH 8.5, T 303 K	[109]
	Sep (M)	-	-	-	161.29	pH 5.0, T 298 K	[110]
	Fe-NPs (M)	Fe ₃ O ₄	DETA (N)	C ₄ H ₁₃ N ₃	141.12	pH 6.0, T 298 K	[111]

q_{max} : Maximum adsorption capacity; (N): nitrogen-based compounds; (O): oxygen-based compounds; (M): metal-based compounds; T: temperature of adsorption test; *: for crosslinkers/covalent linkers that are polymeric, the chemical formula corresponds to the formula of the corresponding monomer.

The results presented in Table 2 can be analysed in terms of the influence of electrostatic forces (also known as Coulombic forces) on the adsorption process of oppositely charged pollutants onto the binding sites [112]. The adsorbent surface enriched with active functional groups contains electron donor elements, acting as adsorptive sites for metal binding [27,113] through chemical interaction (ion exchange, surface complexation and Lewis's acid-base interactions) [112]. Indeed, the use of adsorbents possessing nitrogenous and oxygenated groups (e.g., $-NH_2$, $-OH$, $-COOH$, $-CONH_2$) allows coordination or chemical bonding with heavy metal cations due to the vacant 3d orbital [114,115]. For example, the incorporation of polyethyleneimine (PEI) as a crosslinker into the GO matrix increased the sorption capacity by interacting with As(III) and As(V) through complexation and electrostatic interactions [116], where PEI showed that up to 70% of the polymer links take part in complex formation [117]. However, pH values under 7.8 promote the protonation of $-NH_2$ ($-NH_3^+$) and $-OH$ ($-OH_2^+$) functional groups, then attract anions and repel cations [118]. Moreover, the high concentrations of H^+ and H_3O^+ in solution would compete with HMI to attach to the available binding sites of GO-based nanomaterials, finally reducing the adsorption of metal ions at low pH [119]. The cationic- π binding mechanism involves the non-covalent interaction between a positively charged pollutant and the negatively charged electron cloud of the π system in GO-based sorbents [120].

In the case of GO modified by a metal-based crosslinker, HMI can be adsorbed by forming surface complexes with one, two or multiple binding points [121]. For example, the adsorption of As(V) for GO modified with gadolinium oxide (Gd_2O_3) is mainly due to the electrostatic attraction of carbonyl groups with gadolinium oxide and the electrons of the π - π bounds [122,123]. It has been reported that the adsorption capacity is increased by having oxygenated groups along the surface, and this benefits the porous structure and superparamagnetic properties [124]. Figure 2 summarises the HMI adsorption mechanisms with GO materials functionalised with nitrogen, oxygen and metal compounds, where M^{x+} represents a heavy metal cation and MO_x^{y-} represents a heavy metal anion.

Concerning the chemical structure of crosslinker/covalent linker, the number of binding sites could be considered. For instance, the nitrogen groups have one bonding point (one non-bonding electron pair), the oxygen groups have two bonding points (two non-bonding electron pairs), and the benzene rings of the GO/crosslinker/covalent linker have one bonding point (cation- π interaction). Then, the structure of the functionalised GO can be related to the maximum adsorption capacity of this material. Figure 3 presents the relationship between GO-crosslinker/covalent linker bonding points and the maximum adsorption capacity from the data in Table 2.

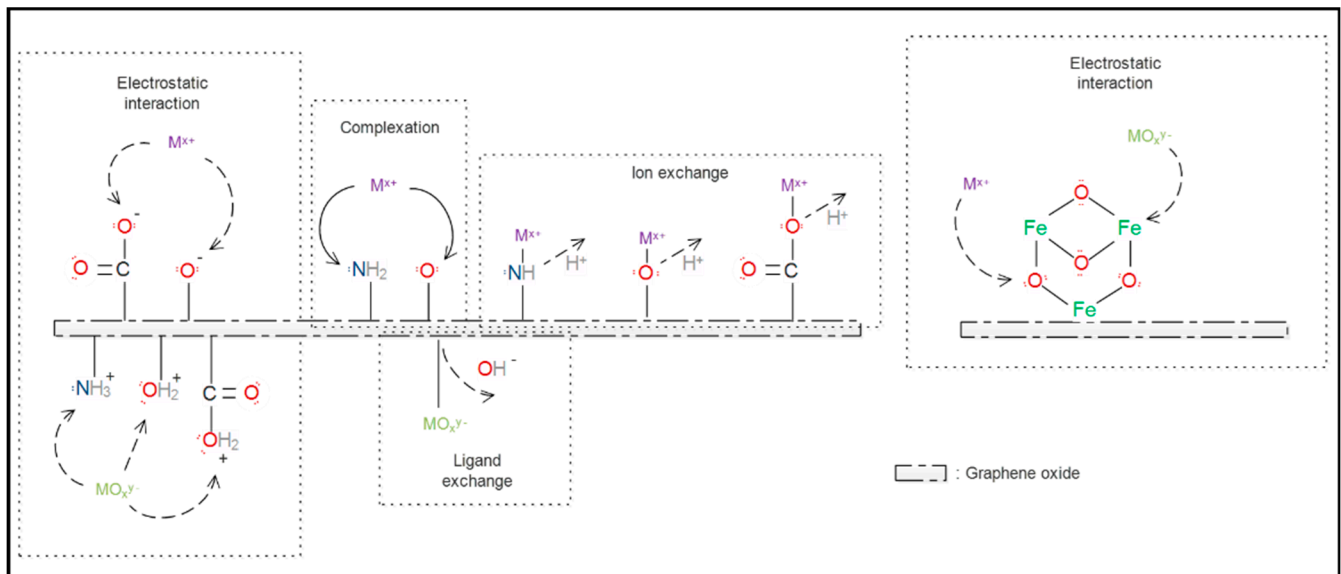


Figure 2. Heavy metal ion adsorption mechanism using GO-based materials functionalised with nitrogenous or oxygenated crosslinker (left) and metal-based crosslinker (right).

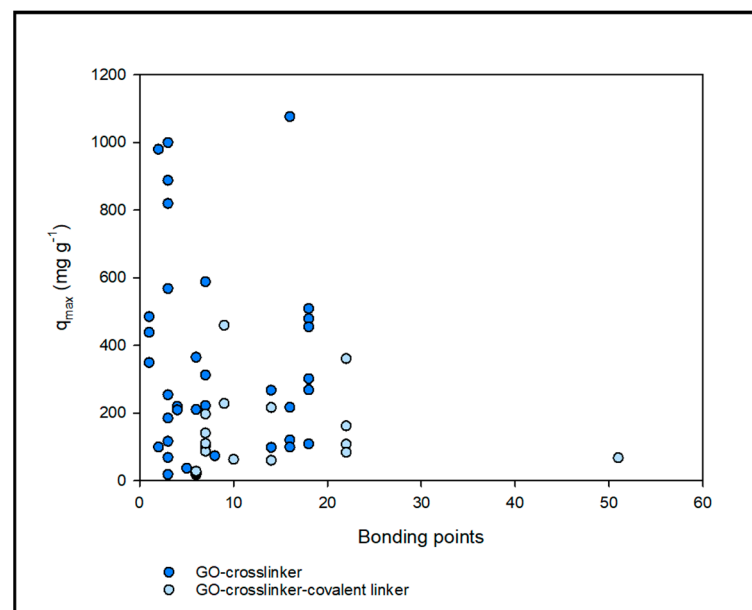


Figure 3. Scatter plot between the bonding points of functionalised GO-based compounds and the maximum adsorption capacity of heavy metal ions.

At first glance, adding the covalent linker decreases the adsorption of HMI despite the higher number of bonding points. Excessive cross-linking not only disrupts and blocks water transport within the GO nanochannels [23], but it can also decrease the adsorption capacity of HMI due to the disruption of binding sites caused by the covalent linker in the GO-cross-linking structure [125]. In addition, the molecular structure of GO-crosslinker-covalent linker adsorbent is generally large and unstable, which leads to structural damage in the adsorption process [126].

4. Separation of Heavy Metal Ion Performance by Modified Graphene Oxide Functionalised Membranes

In membrane separation processes, rejection refers to the ability of a membrane to block specific solutes from passing through, allowing only solvent permeation. Essentially, the

percentage of the solute prevented passage through the membrane. Conversely, flux is the permeate flow rate through the membrane per unit area. These two parameters are essential in understanding the efficiency and effectiveness of the membrane separation processes.

Table 3 presents the HMI rejection of GO membranes modified by different crosslinkers/covalent linkers.

Table 3. Performance and operating conditions of crosslinker and crosslinker-covalent linker-functionalised GO membranes for removing heavy metal ions.

Heavy Metal Ion	Crosslinker (Classification)	Covalent Linker (Classification)	Rejection (%)	Operating Condition	Reference
As(III)	TETA (N)	CuFe ₂ O ₄ (M)	81.2%	4.0 bar	[127]
	QT (O)	-	67.0%	1.0 bar	[128]
As(V)	TETA (N)	CuFe ₂ O ₄ (M)	87.9%	4.0 bar	[127]
	H ₂ SO ₄ (O)	-	79.0%	2.0 bar	[129]
Cd(II)	QT (O)	-	75.0%	1.0 bar	[128]
	IPDI (N)	-	52.8%	1.0 bar	[130]
	PMMA (O)	-	68.0%	5.0 bar	[131]
	EDA (N)	PEI (N)	90.5%	1.0 bar	[132]
Cr(II)	CR (N, O)	Ca ²⁺ (M)	99.5%	5.0 bar	[133]
	POSS (M)	PERI (N)	80.0%	4.5 bar	[134]
Cr(VI)	IPDI (N)	-	71.1%	1.0 bar	[130]
	QT (O)	-	70.0%	1.0 bar	[128]
Cu(II)	H ₂ SO ₄ (O)	-	37.5%	2.0 bar	[129]
	EDA (N)	-	100.0%	21.0 bar	[135]
	MeF (N)	Fe ₃ O ₄ (M)	92.0%	4.0 bar	[136]
	POSS (M)	PERI (N)	55.0%	4.5 bar	[134]
	IPDI (N)	-	46.2%	1.0 bar	[130]
	UR (N, O)	-	81.0%	1.0 bar	[137]
	EDA (N)	-	59.0%	1.0 bar	[137]
	PMMA (O)	-	58.0%	5.0 bar	[131]
	K ⁺ (M)	-	97.5%	1.0 bar	[138]
	Ba ²⁺ (M)	-	96.4%	1.0 bar	
	Ca ²⁺ (M)	-	96.2%	1.0 bar	
	Mg ²⁺ (M)	-	95.7%	1.0 bar	
Ni(II)	CR (N, O)	Ca ²⁺ (M)	99.0%	5.0 bar	[133]
	PMMA (O)	-	73.0%	5.0 bar	[131]
	EDA (N)	PEI (N)	96.0%	1.0 bar	[132]
	K ⁺ (M)	-	94.3%	1.0 bar	[138]
	Ba ²⁺ (M)	-	93.4%	1.0 bar	
	Ca ²⁺ (M)	-	93.3%	1.0 bar	
	Mg ²⁺ (M)	-	92.4%	1.0 bar	
	CR (N, O)	Ca ²⁺ (M)	98.0%	5.0 bar	[133]
Pb(II)	QT (O)	-	74.0%	1.0 bar	[128]
	POSS (M)	PERI (N)	78.0%	4.5 bar	[134]
	IPDI (N)	-	66.4%	1.0 bar	[130]
	EDA (N)	PEI (N)	95.7%	1.0 bar	[132]
	K ⁺ (M)	-	92.2%	1.0 bar	[138]
	Ba ²⁺ (M)	-	91.9%	1.0 bar	
	Ca ²⁺ (M)	-	92.5%	1.0 bar	
	Mg ²⁺ (M)	-	91.2%	1.0 bar	
Zn(II)	CR (N, O)	Ca ²⁺ (M)	98.0%	5.0 bar	[133]
	PMMA (O)	-	79.0%	5.0 bar	[131]
	EDA (N)	PEI (N)	97.4%	1.0 bar	[132]

(N): nitrogen-based compounds; (O): oxygen-based compounds; (M): metal-based compounds.

In general, nitrogenous and oxygenated crosslinkers have been the most widely used for HMI nanofiltration processes because covalent crosslinking between nitrogen-containing (-NH₂) or oxygen-containing functional groups (-OH, -COOH, -COC-) with GO [139], is stronger than the non-covalent crosslinking (Van der Waals forces, hydrophobic

interaction, π - π interactions, electrostatic and hydrogen bonding) of the metal-based crosslinker and GO [23].

Enhancing the hydrophilicity of hydrophobic surfaces has been widely regarded as an effective strategy for improving water permeability [140]. The non-oxidized GO surface and the hydrophilic functional groups of GO induce water molecules to cross the membrane to increase their transfer rate [141,142], such as a “sliding effect”, which is detrimental when treating hydrated ions. Water molecules are generally viewed as vehicles for ion transport in an aqueous environment, which can form a shell around ions with the help of hydrogen bonds [143]. This may result in an increase in ionic flow, which would be controlled by pore size and the transmembrane pressure [144]. On the other hand, Donnan exclusion involves a local equilibrium in the membrane, which results in the exclusion of almost all co-ions at the membrane entrance while counter-ions are absorbed and transported [145]. In the case of HMI, electrostatic attraction between the nanocomposites and cations will occur, while electrostatic repulsion will occur with anions [118]. For example, the introduction of $-\text{NH}_3^+$ groups makes the GO membrane impermeable to Fe^{2+} successfully [143]. This phenomenon can be explained due to the protonation of amine and carboxylic groups of GO functionalised by an N-based crosslinker, which confers to the membrane a positive charge [146].

Figure 4a depicts the box plots for the data presented in Table 3. In the case of HMI rejection, incorporating the covalent linker leads to increased metal ion removal compared to GO-crosslinker-only membranes due to the precise control of interlayer spacing [147,148]. For this reason, the rejection of GO-crosslinker-covalent linker membranes is higher than that of GO-crosslinker membranes.

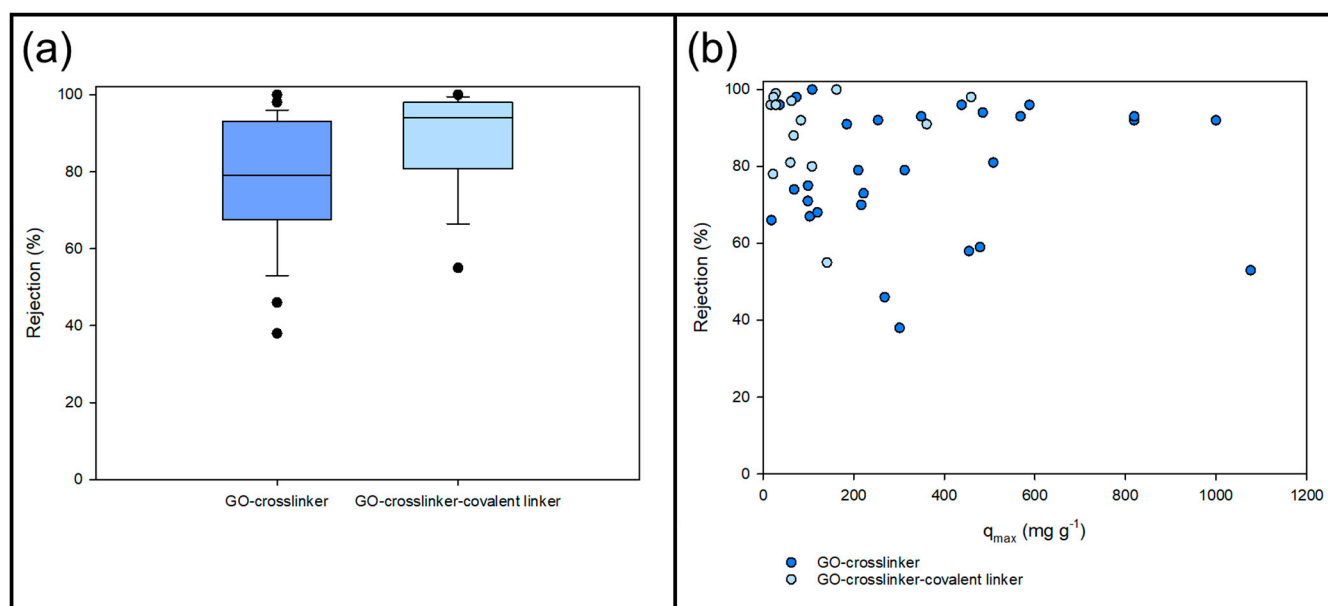


Figure 4. (a) Box plots for rejection of heavy metal ions with functionalised GO membranes; (b) relationship between the maximum adsorption capacity of GO-crosslinker/covalent linker and the rejection of heavy metal ions.

The following question arises from the previous section: can the performance of functionalised GO membranes be related to the adsorption of metal contaminants? Figure 4b presents the relationship between the maximum adsorption capacity of GO-crosslinker/covalent linker and the rejection of HMI with these membranes. Membranes with GO-crosslinker-covalent linkers show a lower adsorption capacity, but higher HMI rejection than functionalised GO with a crosslinker. However, there is a need to study what happens in pollutant removal processes with functionalised GO membranes.

5. Phenomenological Aspects of the Membrane Separation Process

Several principal equations are commonly used to describe and analyse the phenomena involved in membrane separation processes. Equation (1) describes the three transport mechanisms involved simultaneously in the nanofiltration process for ionic solutes: diffusion, convection, and electro-migration [149]. All equations use S.I. units.

$$J_i = -D_{i,p} \cdot \nabla c_i + K_{i,c} \cdot c_i \cdot J_p - \frac{z_i \cdot F}{R \cdot T} \cdot D_{i,p} \cdot c_i \cdot \nabla \psi \quad (1)$$

where J_i is the flux per unit area of ion i , $D_{i,p}$ is the diffusivity of species i within the membrane pore, c_i is the concentration of species i in the pore, z_i is the valence of species i , R is the universal gas constant, T is the absolute temperature, F is Faraday's constant, ψ is the Donnan potential of the membrane, $K_{i,c}$ is the hindrance factor for the convective term and J_p is the permeate flow rate. To determinate $D_{i,p}$, this can be calculated by Equation (2).

$$D_{i,p} = K_{i,d} \cdot D_{i,\infty} \quad (2)$$

where $D_{i,\infty}$ is the diffusivity of species i in the bulk solvent, $K_{i,d}$ is the hindrance factor for the diffusive term. The hindrance factors $K_{i,d}$ and $K_{i,c}$ are functions of the ratio between the solute radius (r_i) and the membrane pore radius (r_p) (Equation (3)).

$$\lambda = \frac{r_i}{r_p} \quad (3)$$

Equations (4) and (5) allow for the determining of hindrance factors for $0 < \lambda < 0.8$.

$$K_{i,d} = 1.0 - 2.30 \cdot \lambda + 1.154 \cdot \lambda^2 + 0.224 \cdot \lambda^3 \quad (4)$$

$$K_{i,c} = (2 - \Phi) \cdot (1.0 + 0.054 \cdot \lambda - 0.998 \cdot \lambda^2 + 0.441 \lambda^3) \quad (5)$$

where Φ is the steric partition coefficient, representing the likelihood of a solute, smaller than the pore, successfully entering the pore (Equation (6)).

$$\Phi = \begin{cases} (1 - \lambda)^2, & r_i < r_p \\ 0, & r_i \geq r_p \end{cases} \quad (6)$$

Regarding the electroneutrality principle and electrostatic interaction between solutes and membrane pores, the Poisson–Nernst–Planck (PNP) equation determines the change in ion concentration over time (Equation (7)) [150]. This equation could be used to predict the content of metal ions in both the membrane structure and the permeate by a mass balance.

$$\frac{\partial c_i}{\partial t} + \nabla \cdot J_i = 0 \quad (7)$$

Replacing Equation (1) in Equation (7), we obtain Equation (8).

$$\frac{\partial c_i}{\partial t} = D_{i,p} \cdot \nabla^2 c_i + K_{i,c} \cdot (c_i \cdot \nabla J_p + \nabla c_i \cdot J_p) - \frac{z_i \cdot F}{R \cdot T} \cdot D_{i,p} \cdot (\nabla c_i \cdot \nabla \psi + c_i \cdot \nabla^2 \psi) \quad (8)$$

Regarding Donnan potential, if the electric potential gradient is uniform for all ions within the membrane, this gradient results in Equation (9) [149]:

$$\nabla \psi = \frac{\sum_{i=1}^n \left(\frac{z_i \cdot J_p}{D_{i,p}} \cdot (K_{i,c} \cdot c_i - C_{i,p}) \right)}{\frac{F}{RT} \cdot \sum_{i=1}^n n(z_i^2 \cdot c_i)} \quad (9)$$

where $C_{i,p}$ is the concentration of the species i in the permeate. Considering that Donnan potential is usually very low ($\nabla\psi \approx 0$), the system is an incompressible fluid ($\nabla J_p = 0$), and $\nabla^2\psi$ can be calculated by Equation (10), and Equation (8) is reduced to Equation (11).

$$\nabla^2\psi = -\frac{\rho_e}{\varepsilon} \quad (10)$$

$$\frac{\partial c_i}{\partial t} = D_{i,p} \cdot \nabla^2 c_i - K_{i,c} \cdot J_p \cdot \nabla c_i + \frac{z_i \cdot F}{R \cdot T} \cdot D_{i,p} \cdot \frac{\rho_e}{\varepsilon} \cdot c_i \quad (11)$$

where ρ_e is the charge density, and ε is the permittivity of the membrane. The change in concentration in the permeate would be related to adsorption by means of the charge density. Zhang et al. [151] investigate the effect of layer charge density and cation concentration on the structures and dynamics of Pb^{2+} , Ba^{2+} and Cs^+ adsorbed in the interlayer and nanopore of montmorillonite. The results show that the higher the charge density, the higher the adsorption amount. Therefore, there is a direct relationship between metal adsorption and charge density [152], e.g., Kalaitzidou et al. [153] determined that the adsorption capacity of iron oxy-hydroxides (FeOOH) for $\text{Se}(\text{IV})$ is strongly related to positive surface charge density when the metal is as SeO_3^{2-} and increases when synthesis pH is lowered (more positive surface charge density).

On the other hand, Osorio et al. [154] proposed a model to determinate the relationship between membrane charge density and cation concentration, where the membrane charge density is defined as a function of the local concentration of divalent cations (Equation (12)).

$$\rho_e = \rho_{e,0} \cdot \frac{1 - K_b \cdot c_i}{1 + K_b \cdot c_i} \quad (12)$$

where c_i —concentration of divalent cation, K_b —the membrane-cation binding constant and $\rho_{e,0}$ —the bare membrane charge density (the charge in the absence of cations in solution). Additionally, Li et al. [155] demonstrated by means of molecular dynamics simulations that the higher the surface charge density, the greater the passage of metal ions in graphene membranes. This provides a direct relationship between the surface charge density and the permeate of metal ions, which is described by Equation (11).

Another model for determining the surface charge density is by correlating the bulk ion concentration with the membrane surface charge density through the Freundlich-type isotherm. This model is acceptable at low electrolyte concentrations, but for real-life brackish or saline water, the bulk concentration is quite high [156]. Finally, the zeta potential can be used to measure the membrane charge density. Then, the charge density can then be incorporated into a model based on the Teorell–Meyer–Sievers theory to calculate the rejection of nanofiltration membranes under the assumption of constant membrane potential [157].

In summary, the phenomenological analysis shows that an increase in surface charge density leads to increased adsorption and flux of metal ions in functionalised GO membrane systems, thus reducing the membrane selectivity. This concurs with the experimental data collected and displayed in Figure 3. However, there are no studies in the literature that relate the characteristics of the functionalising compound (crosslinker and covalent linker) to the surface charge density and, consequently, to the adsorption and permeation of heavy metal ions. Under this logic, it is recommended to study the effects that crosslinkers or covalent linkers would have considering Equations (1)–(12). In addition, it is known that membrane desorption and regeneration cause secondary pollution [158] and the decrease in adsorption performance due to the loss of adsorbent material during multiple cycles [159], the dissolution of adsorbent in the treated flow [160] or the loss of functional groups [161]. So, it is necessary to study the enhanced reuse of functionalized GO membranes and the final disposal of the waste generated.

6. Conclusions

Membrane separation includes the linked phenomenon of adsorption and filtration; this fact is confirmed after an analysis of published results with modified graphene oxide-functionalised inorganic membrane. In this material separation, performance depends on the hydrophobic interactions of the membrane and the solute [162].

The underlying mechanism that governs the interaction between graphene oxide membrane and heavy metal ions is directly linked with the adsorption phenomena through different mechanisms, including both ionic and coordinative interaction and metal complexation with oxygenate functional groups. These interactions are affected by the chemical modification arising from the functionalization procedures.

The nature of the crosslinker directly affects the performance of functionalised GO membranes, where the adsorption of heavy metal ions is determined by the attachment points of the crosslinker.

Adsorption of heavy metal ions changes the charge density of the membrane, leading to an increase in ions in the permeate. Depending on the material, the change in charge density will be different.

Further research effort is still necessary to obtain a complete description of the relationship between nanofiltration and HMI adsorption performance when using inorganic GO-functionalised membranes that have been modified with different crosslinkers to offer a predictive tool for designing new materials.

This predictive tool must support the development of many relevant areas which need more research for massive industrial applications of the inorganic functionalised membrane technology, such as improved life cycle and recyclability, scalable commercial manufacturing and the real-scale demonstration of the energetic benefits in comparison of dense polymeric membranes.

Funding: This work has been funded by the project InES I+D PUCV código INID230010.

Acknowledgments: M. Ayala-Claveria acknowledges the PUCV master scholarship.

Conflicts of Interest: The authors declare no conflict of interest.

Nomenclature

Abbreviation	Name
APTES	3-aminopropyltriethoxysilane
ATP	4-aminothiophenol
CDx	Cyclodextrin
Co-NPs	Co nanoparticles
CR	Congo Red
CS	Chitosan
CuFe ₂ O ₄	Copper ferrite
DACHTA	1,2-diaminocyclohexanetetraacetic acid
DETA	Diethylenetriamine
EDA	Ethylenediamine
EDTA	Ethylene diamine tetraacetic acid
Fe-NPs	Fe nanoparticles
Gly	Glycine
HPA	Hyperbranched polyamine
HPEI	Hyperbranched polyethyleneimine
IPDI	Isophorone diisocyanate
Lc-Al ₂ O ₃	Lignocellulosic-Al ₂ O ₃ hybrid biosorbent
L-Cys	L-cysteine
LL-NaOH	Leucaena leucephala treated with NaOH

LS	Lignosulfonated
L-Trp	L-tryptophan
LVB	Lagenaria vulgaris biosorbent
MeF	Metformin
MgAl-LDH	MgAl-layered double hydroxides
OPhDA	Ortophenylenediamine
PAAm	Polyallylamine
PAM	Polyacrylamide
PANI	Polyaniline
PDA	Polydopamine
PEI	Polyethyleneimine
PERI	Polyetherimide
PMMA	Hydrolyzed polymethylmethacrylate
POSS	Octa glycidylxypropyl-silsesquioxane
PPhDA	Paraphenylenediamine
PPy	Polypyrrole
PVK	Poly(N-vinylcarbazole)
QT	Quercetin
SA	Sodium alginate
SAC	Sulfanilic acid
Sep	Sepiolite
TETA	Triethylenetetramine
TNRs	Titanate nanorings
UR	Urea
Ze-nWRT	Zeolite functionalised with nanostructured water treatment residual
ZIF-8-EDA	Zeolite imidazolate framework-8 functionalised with ethylenediamine

References

- Nujić, M.; Habuda-Stanić, M. Toxic metal ions in drinking water and effective removal using graphene oxide nanocomposite. In *A New Generation Material Graphene: Applications in Water Technology*; Springer International Publishing: Berlin/Heidelberg, Germany, 2018; pp. 373–395. [\[CrossRef\]](#)
- Jaishankar, M.; Tseten, T.; Anbalagan, N.; Mathew, B.B.; Beeregowda, K.N. Toxicity, mechanism and health effects of some heavy metals. *Interdiscip. Toxicol.* **2014**, *7*, 60–72. [\[CrossRef\]](#) [\[PubMed\]](#)
- Shrestha, R.; Ban, S.; Devkota, S.; Sharma, S.; Joshi, R.; Tiwari, A.P.; Kim, H.Y.; Joshi, M.K. Technological trends in heavy metals removal from industrial wastewater: A review. *J. Environ. Chem. Eng.* **2021**, *9*, 105688. [\[CrossRef\]](#)
- Qiu, Y.; Depuydt, S.; Ren, L.F.; Zhong, C.; Wu, C.; Shao, J.; Xia, L.; Zhao, Y.; Van der Bruggen, B. Progress of Ultrafiltration-Based Technology in Ion Removal and Recovery: Enhanced Membranes and Integrated Processes. *ACS ES&T Water* **2022**, *3*, 1702–1719. [\[CrossRef\]](#)
- Fu, F.; Wang, Q. Removal of heavy metal ions from wastewaters: A review. *J. Environ. Manag.* **2011**, *92*, 407–418. [\[CrossRef\]](#)
- Burakov, A.E.; Galunin, E.V.; Burakova, I.V.; Kucherova, A.E.; Agarwal, S.; Tkachev, A.G.; Gupta, V.K. Adsorption of heavy metals on conventional and nanostructured materials for wastewater treatment purposes: A review. *Ecotoxicol. Environ. Saf.* **2018**, *148*, 702–712. [\[CrossRef\]](#)
- Nompumelelo, K.S.M.; Edward, N.N.; Muthumuni, M.; Moloko, M.; Makwena, M.J. Fabrication, Modification, and Mechanism of Nanofiltration Membranes for the Removal of Heavy Metal Ions from Wastewater. *ChemistrySelect* **2023**, *8*, e202300741. [\[CrossRef\]](#)
- Mohsen-Nia, M.; Montazeri, P.; Modarress, H. Removal of Cu²⁺ and Ni²⁺ from wastewater with a chelating agent and reverse osmosis processes. *Desalination* **2007**, *217*, 276–281. [\[CrossRef\]](#)
- Zhang, L.; Wu, Y.; Qu, X.; Li, Z.; Ni, J. Mechanism of combination membrane and electro-winning process on treatment and remediation of Cu²⁺ polluted water body. *J. Environ. Sci.* **2009**, *21*, 764–769. [\[CrossRef\]](#)
- Chan, B.K.C.; Dudeney, A.W.L. Reverse osmosis removal of arsenic residues from bioleaching of refractory gold concentrates. *Miner. Eng.* **2008**, *21*, 272–278. [\[CrossRef\]](#)
- Ipek, U. Removal of Ni(II) and Zn(II) from an aqueous solution by reverse osmosis. *Desalination* **2005**, *174*, 161–169. [\[CrossRef\]](#)
- Zhao, M.; Xu, Y.; Zhang, C.; Rong, H.; Zeng, G. New trends in removing heavy metals from wastewater. *Appl. Microbiol. Biotechnol.* **2016**, *100*, 6509–6518. [\[CrossRef\]](#) [\[PubMed\]](#)
- El Batouti, M.; Al-Harby, N.F.; Elewa, M.M. A Review on Promising Membrane Technology Approaches for Heavy Metal Removal from Water and Wastewater to Solve Water Crisis. *Water* **2021**, *13*, 3241. [\[CrossRef\]](#)
- Ezugbe, E.O.; Rathilal, S. Membrane technologies in wastewater treatment: A review. *Membranes* **2020**, *10*, 89. [\[CrossRef\]](#)
- Zhang, Y.; Tan, Y.; Sun, R.; Zhang, W. Preparation of Ceramic Membranes and Their Application in Wastewater and Water Treatment. *Water* **2023**, *15*, 3344. [\[CrossRef\]](#)

16. Goh, P.S.; Ismail, A.F. A review on inorganic membranes for desalination and wastewater treatment. *Desalination* **2018**, *434*, 60–80. [[CrossRef](#)]
17. Fard, A.K.; McKay, G.; Buekenhoudt, A.; Al Sulaiti, H.; Motmans, F.; Khraisheh, M.; Atieh, M. Inorganic membranes: Preparation and application for water treatment and desalination. *Materials* **2018**, *11*, 74. [[CrossRef](#)]
18. Kotobuki, M.; Gu, Q.; Zhang, L.; Wang, J. Ceramic-Polymer Composite Membranes for Water and Wastewater Treatment: Bridging the Big Gap between Ceramics and Polymers. *Molecules* **2021**, *26*, 3331. [[CrossRef](#)]
19. Samaei, S.M.; Gato-Trinidad, S.; Altaee, A. The application of pressure-driven ceramic membrane technology for the treatment of industrial wastewaters—A review. *Sep. Purif. Technol.* **2018**, *200*, 198–220. [[CrossRef](#)]
20. Ma, Y.; Zheng, Y.; Zhu, Y. Towards industrialization of graphene oxide. *Sci. China Mater.* **2020**, *63*, 1861–1869. [[CrossRef](#)]
21. Pedico, A.; Baudino, L.; Aixalà-Perelló, A.; Lamberti, A. Green Methods for the Fabrication of Graphene Oxide Membranes: From Graphite to Membranes. *Membranes* **2023**, *13*, 429. [[CrossRef](#)]
22. Tian, L.; Zhou, P.; Graham, N.; Li, G.; Yu, W. Long-term operation and biofouling of graphene oxide membrane in practical water treatment: Insights from performance and biofilm characteristics. *J. Memb. Sci.* **2023**, *680*, 121761. [[CrossRef](#)]
23. Wang, Z.; He, F.; Guo, J.; Peng, S.; Cheng, X.Q.; Zhang, Y.; Drioli, E.; Figoli, A.; Li, Y.; Shao, L. The stability of a graphene oxide (GO) nanofiltration (NF) membrane in an aqueous environment: Progress and challenges. *Mater. Adv.* **2020**, *1*, 554–568. [[CrossRef](#)]
24. Abdullah, N.; Yusof, N.; Lau, W.J.; Jaafar, J.; Ismail, A.F. Recent trends of heavy metal removal from water/wastewater by membrane technologies. *J. Ind. Eng. Chem.* **2019**, *76*, 17–38. [[CrossRef](#)]
25. Xiang, H.; Min, X.; Tang, C.J.; Sillanpää, M.; Zhao, F. Recent advances in membrane filtration for heavy metal removal from wastewater: A mini review. *J. Water Process Eng.* **2022**, *49*, 103023. [[CrossRef](#)]
26. Abadi, P.G.S.; Irani, M.; Rad, L.R. Mechanisms of the removal of the metal ions, dyes, and drugs from wastewaters by the electrospun nanofiber membranes. *J. Taiwan. Inst. Chem. Eng.* **2023**, *143*, 104625. [[CrossRef](#)]
27. Liu, X.; Ma, R.; Wang, X.; Ma, Y.; Yang, Y.; Zhuang, L.; Zhang, S.; Jehan, R.; Chen, J.; Wang, X. Graphene oxide-based materials for efficient removal of heavy metal ions from aqueous solution: A review. *Environ. Pollut.* **2019**, *252*, 62–73. [[CrossRef](#)]
28. Li, W.; Mu, B.; Yang, Y. Feasibility of industrial-scale treatment of dye wastewater via bio-adsorption technology. *Bioresour. Technol.* **2019**, *277*, 157–170. [[CrossRef](#)]
29. Šljivić, M.; Smičiklas, I.; Pejanović, S.; Plećaš, I. Comparative study of Cu²⁺ adsorption on a zeolite, a clay and a diatomite from Serbia. *Appl. Clay Sci.* **2009**, *43*, 33–40. [[CrossRef](#)]
30. Sitko, R.; Turek, E.; Zawisza, B.; Malicka, E.; Talik, E.; Heimann, J.; Gagor, A.; Feist, B.; Wrzalik, R. Adsorption of divalent metal ions from aqueous solutions using graphene oxide. *Dalton Trans.* **2013**, *42*, 5682–5689. [[CrossRef](#)]
31. Khosravi, A.; Habibpour, R.; Ranjbar, M. Enhanced adsorption and removal of Cd(II) from aqueous solution by amino-functionalized ZIF-8. *Sci. Rep.* **2024**, *14*, 10736. [[CrossRef](#)]
32. Manousi, N.; Rosenberg, E.; Deliyanni, E.A.; Zachariadis, G.A. Sample preparation using graphene-oxide-derived nanomaterials for the extraction of metals. *Molecules* **2020**, *25*, 2411. [[CrossRef](#)] [[PubMed](#)]
33. Peng, W.; Li, H.; Liu, Y.; Song, S. A review on heavy metal ions adsorption from water by graphene oxide and its composites. *J. Mol. Liq.* **2017**, *230*, 496–504. [[CrossRef](#)]
34. Sengupta, S.; Pari, A.; Biswas, L.; Shit, P.; Bhattacharyya, K.; Chattopadhyay, A.P. Adsorption of arsenic on graphene oxide, reduced graphene oxide, and their Fe₃O₄ doped nanocomposites. *Biointerface Res. Appl. Chem.* **2022**, *12*, 6196–6210. [[CrossRef](#)]
35. Tolkou, A.K.; Rada, E.C.; Torretta, V.; Xanthopoulou, M.; Kyzas, G.Z.; Katsoyiannis, I.A. Removal of Arsenic(III) from Water with a Combination of Graphene Oxide (GO) and Granular Ferric Hydroxide (GFH) at the Optimum Molecular Ratio. *J. Carbon. Res.* **2023**, *9*, 10. [[CrossRef](#)]
36. Liu, L.; Li, C.; Bao, C.; Jia, Q.; Xiao, P.; Liu, X.; Zhang, Q. Preparation and characterization of chitosan/graphene oxide composites for the adsorption of Au(III) and Pd(II). *Talanta* **2012**, *93*, 350–357. [[CrossRef](#)] [[PubMed](#)]
37. Tan, P.; Sun, J.; Hu, Y.; Fang, Z.; Bi, Q.; Chen, Y.; Cheng, J.; Cu, A.O. Cd²⁺ and Ni²⁺ from aqueous single metal solutions on graphene oxide membranes. *J. Hazard. Mater.* **2015**, *297*, 251–260. [[CrossRef](#)] [[PubMed](#)]
38. Elkhatib, E.A.; Moharem, M.L.; Saad, A.F.; Abdelhamed, S. A novel nanocomposite-based zeolite for efficient remediation of Cd-contaminated industrial wastewater. *Appl. Water Sci.* **2024**, *14*, 75. [[CrossRef](#)]
39. Lingamdinne, L.P.; Koduru, J.R.; Roh, H.; Choi, Y.L.; Chang, Y.Y.; Yang, J.K. Adsorption removal of Co(II) from waste-water using graphene oxide. *Hydrometallurgy* **2016**, *165*, 90–96. [[CrossRef](#)]
40. Abatal, M.; Lima, E.C.; Anastopoulos, I.; Giannakoudakis, D.A.; Vargas, J.; Aguilar, C.; Olguín, M.T.; Anguebes-Fransechi, F. Effect of alkali treatment on the removal of Co(II) ions by *Leucaena leucecephala* biomass. *J. Mol. Liq.* **2022**, *367*, 120419. [[CrossRef](#)]
41. Mondal, N.K.; Chakraborty, S. Adsorption of Cr(VI) from aqueous solution on graphene oxide (GO) prepared from graphite: Equilibrium, kinetic and thermodynamic studies. *Appl. Water Sci.* **2020**, *10*, 61. [[CrossRef](#)]
42. Yang, S.T.; Chang, Y.; Wang, H.; Liu, G.; Chen, S.; Wang, Y.; Liu, Y.; Cao, A. Folding/aggregation of graphene oxide and its application in Cu²⁺ removal. *J. Colloid. Interface Sci.* **2010**, *351*, 122–127. [[CrossRef](#)] [[PubMed](#)]
43. Wu, W.; Yang, Y.; Zhou, H.; Ye, T.; Huang, Z.; Liu, R.; Kuang, Y. Highly efficient removal of Cu(II) from aqueous solution by using graphene oxide. *Water Air Soil. Pollut.* **2013**, *224*, 1372. [[CrossRef](#)]
44. Velinov, N.; Mitrović, J.; Kostić, M.; Radović, M.; Petrović, M.; Bojić, D.; Bojić, A. Wood residue reuse for a synthesis of lignocellulosic biosorbent: Characterization and application for simultaneous removal of copper (II), Reactive Blue 19 and cyprodinil from water. *Wood Sci. Technol.* **2019**, *53*, 619–647. [[CrossRef](#)]

45. Kostić, M.M.; Radović, M.D.; Mitrović, J.Z.; Bojić, D.V.; Milenković, D.D.; Bojić, A.L. Application of new biosorbent based on chemically modified *Lagenaria vulgaris* shell for the removal of copper(II) from aqueous solutions: Effects of operational parameters. *Hem. Ind.* **2013**, *67*, 559–567. [[CrossRef](#)]
46. Sun, Y.; Wang, Q.; Chen, C.; Tan, X.; Wang, X. Interaction between Eu(III) and graphene oxide nanosheets investigated by batch and extended X-ray absorption fine structure spectroscopy and by modeling techniques. *Environ. Sci. Technol.* **2012**, *46*, 6020–6027. [[CrossRef](#)] [[PubMed](#)]
47. Zheng, M.; Ji, H.; Duan, J.; Dang, C.; Chen, X.; Liu, W. Efficient adsorption of europium (III) and uranium (VI) by titanate nanorings: Insights into radioactive metal species. *Environ. Sci. Ecotechnology* **2020**, *2*, 100031. [[CrossRef](#)]
48. Tene, T.; Bellucci, S.; Guevara, M.; Arias, F.A.; Paguay, M.Á.S.; Moyota, J.M.Q.; Polanco, M.A.; Scarcello, A.; Gomez, C.V.; Straface, S.; et al. Adsorption of Mercury on Oxidized Graphenes. *Nanomaterials* **2022**, *12*, 3025. [[CrossRef](#)]
49. Leiva, E.; Tapia, C.; Rodríguez, C. Removal of Mn(II) from Acidic Wastewaters Using Graphene Oxide–ZnO Nanocomposites. *Molecules* **2021**, *26*, 2713. [[CrossRef](#)]
50. Najafi, F.; Moradi, O.; Rajabi, M.; Asif, M.; Tyagi, I.; Agarwal, S.; Gupta, V.K. Thermodynamics of the adsorption of nickel ions from aqueous phase using graphene oxide and glycine functionalized graphene oxide. *J. Mol. Liq.* **2015**, *208*, 106–113. [[CrossRef](#)]
51. Yari, M.; Rajabi, M.; Moradi, O.; Yari, A.; Asif, M.; Agarwal, S.; Gupta, V.K. Kinetics of the adsorption of Pb(II) ions from aqueous solutions by graphene oxide and thiol functionalized graphene oxide. *J. Mol. Liq.* **2015**, *209*, 50–57. [[CrossRef](#)]
52. Zhao, G.; Ren, X.; Gao, X.; Tan, X.; Li, J.; Chen, C.; Huang, Y.; Wang, X. Removal of Pb(II) ions from aqueous solutions on few-layered graphene oxide nanosheets. *Dalton Trans.* **2011**, *40*, 10945–10952. [[CrossRef](#)]
53. Leng, Y.; Guo, W.; Su, S.; Yi, C.; Xing, L. Removal of antimony(III) from aqueous solution by graphene as an adsorbent. *Chem. Eng. J.* **2012**, *212*, 406–411. [[CrossRef](#)]
54. Zhao, Y.; Guo, C.; Fang, H.; Jiang, J. Competitive adsorption of Sr(II) and U(VI) on graphene oxide investigated by batch and modeling techniques. *J. Mol. Liq.* **2016**, *222*, 263–267. [[CrossRef](#)]
55. Xu, H.; Li, G.; Li, J.; Chen, C.; Ren, X.; Th, I.O. Interaction of Th(IV) with graphene oxides: Batch experiments, XPS investigation, and modeling. *J. Mol. Liq.* **2016**, *213*, 58–68. [[CrossRef](#)]
56. Li, Z.; Chen, F.; Yuan, L.; Liu, Y.; Zhao, Y.; Chai, Z.; Shi, W. Uranium(VI) adsorption on graphene oxide nanosheets from aqueous solutions. *Chem. Eng. J.* **2012**, *210*, 539–546. [[CrossRef](#)]
57. Wang, H.; Yuan, X.; Wu, Y.; Huang, H.; Zeng, G.; Liu, Y.; Wang, X.; Lin, N.; Qi, Y. Adsorption characteristics and behaviors of graphene oxide for Zn(II) removal from aqueous solution. *Appl. Surf. Sci.* **2013**, *279*, 432–440. [[CrossRef](#)]
58. Liu, L.; Luo, X.B.; Ding, L.; Luo, S.L. Application of Nanotechnology in the Removal of Heavy Metal from Water. In *Nanomaterials for the Removal of Pollutants and Resource Reutilization*; Elsevier: Amsterdam, The Netherlands, 2019; pp. 83–147. [[CrossRef](#)]
59. Jia, Z.; Wang, Y. Covalently crosslinked graphene oxide membranes by esterification reactions for ions separation. *J. Mater. Chem. A Mater.* **2015**, *3*, 4405–4412. [[CrossRef](#)]
60. Jia, Z.; Shi, W. Tailoring permeation channels of graphene oxide membranes for precise ion separation. *Carbon* **2016**, *101*, 290–295. [[CrossRef](#)]
61. Hung, W.S.; Tsou, C.H.; De Guzman, M.; An, Q.F.; Liu, Y.L.; Zhang, Y.M.; Hu, C.C.; Lee, K.R.; Lai, J.Y. Cross-linking with diamine monomers to prepare composite graphene oxide-framework membranes with varying d-spacing. *Chem. Mater.* **2014**, *26*, 2983–2990. [[CrossRef](#)]
62. Hua, D.; Rai, R.K.; Zhang, Y.; Chung, T.S. Aldehyde functionalized graphene oxide frameworks as robust membrane materials for pervaporative alcohol dehydration. *Chem. Eng. Sci.* **2017**, *161*, 341–349. [[CrossRef](#)]
63. Wei, Y.; Pastuovic, Z.; Shen, C.; Murphy, T.; Gore, D.B. Ion beam engineered graphene oxide membranes for mono-/di-valent metal ions separation. *Carbon* **2020**, *158*, 598–606. [[CrossRef](#)]
64. Lv, X.B.; Xie, R.; Ji, J.Y.; Liu, Z.; Wen, X.Y.; Liu, L.Y.; Hu, J.Q.; Ju, X.J.; Wang, W.; Chu, L.Y. A Novel Strategy to Fabricate Cation-Cross-linked Graphene Oxide Membrane with High Aqueous Stability and High Separation Performance. *ACS Appl. Mater. Interfaces* **2020**, *12*, 56269–56280. [[CrossRef](#)] [[PubMed](#)]
65. Qian, L.; Wang, H.; Yang, J.; Chen, X.; Chang, X.; Nan, Y.; He, Z.; Hu, P.; Wu, W.; Liu, T. Amino acid cross-linked graphene oxide membranes for metal ions permeation, insertion and antibacterial properties. *Membranes* **2020**, *10*, 296. [[CrossRef](#)]
66. Alkhouzaam, A.; Qiblawey, H. Functional GO-based membranes for water treatment and desalination: Fabrication methods, performance and advantages. A review. *Chemosphere* **2021**, *274*, 129853. [[CrossRef](#)]
67. Nan, Q.; Li, P.; Cao, B. Fabrication of positively charged nanofiltration membrane via the layer-by-layer assembly of graphene oxide and polyethylenimine for desalination. *Appl. Surf. Sci.* **2016**, *387*, 521–528. [[CrossRef](#)]
68. Shao, F.; Xu, C.; Ji, W.; Dong, H.; Sun, Q.; Yu, L.; Dong, L. Layer-by-layer self-assembly TiO₂ and graphene oxide on polyamide reverse osmosis membranes with improved membrane durability. *Desalination* **2017**, *423*, 21–29. [[CrossRef](#)]
69. Liu, H.; Pang, X.; Ding, W.; Guo, S.; Ding, Z. Preparation of nano-SiO₂ modified graphene oxide and its application in polyacrylate emulsion. *Mater. Today Commun.* **2021**, *27*, 102245. [[CrossRef](#)]
70. Chen, L.; Shi, G.; Shen, J.; Peng, B.; Zhang, B.; Wang, Y.; Bian, F.; Wang, J.; Li, D.; Qian, Z.; et al. Ion sieving in graphene oxide membranes via cationic control of interlayer spacing. *Nature* **2017**, *550*, 380–383. [[CrossRef](#)]
71. Kong, Q.; Preis, S.; Li, L.; Luo, P.; Wei, C.; Li, Z.; Hu, Y.; Wei, C. Relations between metal ion characteristics and adsorption performance of graphene oxide: A comprehensive experimental and theoretical study. *Sep. Purif. Technol.* **2020**, *232*, 115956. [[CrossRef](#)]

72. Peng, F.; Luo, T.; Qiu, L.; Yuan, Y. An easy method to synthesize graphene oxide–FeOOH composites and their potential application in water purification. *Mater. Res. Bull.* **2013**, *48*, 2180–2185. [[CrossRef](#)]
73. Zhang, F.; Wang, B.; He, S.; Man, R. Preparation of Graphene-Oxide/Polyamidoamine Dendrimers and Their Adsorption Properties toward Some Heavy Metal Ions. *J. Chem. Eng. Data* **2014**, *59*, 1719–1726. [[CrossRef](#)]
74. Dong, Z.; Zhang, F.; Wang, D.; Liu, X.; Jin, J. Polydopamine-mediated surface-functionalization of graphene oxide for heavy metal ions removal. *J. Solid. State Chem.* **2015**, *224*, 88–93. [[CrossRef](#)]
75. Guo, X.; Du, B.; Wei, Q.; Yang, J.; Hu, L.; Yan, L.; Xu, W. Synthesis of amino functionalized magnetic graphenes composite material and its application to remove Cr(VI), Pb(II), Hg(II), Cd(II) and Ni(II) from contaminated water. *J. Hazard. Mater.* **2014**, *278*, 211–220. [[CrossRef](#)] [[PubMed](#)]
76. Cheng, C.; Li, S.; Zhao, J.; Li, X.; Liu, Z.; Ma, L.; Zhang, X.; Sun, S.; Zhao, C. Biomimetic assembly of polydopamine-layer on graphene: Mechanisms, versatile 2D and 3D architectures and pollutant disposal. *Chem. Eng. J.* **2013**, *228*, 468–481. [[CrossRef](#)]
77. Gao, H.; Sun, Y.; Zhou, J.; Xu, R.; Duan, H. Mussel-inspired synthesis of polydopamine-functionalized graphene hydrogel as reusable adsorbents for water purification. *ACS Appl. Mater. Interfaces* **2013**, *5*, 425–432. [[CrossRef](#)]
78. Fang, F.; Kong, L.; Huang, J.; Wu, S.; Zhang, K.; Wang, X.; Sun, B.; Jin, Z.; Wang, J.; Huang, X.J.; et al. Removal of cobalt ions from aqueous solution by an amination graphene oxide nanocomposite. *J. Hazard. Mater.* **2014**, *270*, 1–10. [[CrossRef](#)]
79. Yuan, X.; Wang, Y.; Wang, J.; Zhou, C.; Tang, Q.; Rao, X. Calcined graphene/MgAl-layered double hydroxides for enhanced Cr(VI) removal. *Chem. Eng. J.* **2013**, *221*, 204–213. [[CrossRef](#)]
80. Jabeen, H.; Chandra, V.; Jung, S.; Lee, J.W.; Kim, K.S.; Kim, S.B. Enhanced Cr(VI) removal using iron nanoparticle decorated graphene. *Nanoscale* **2011**, *3*, 3583–3585. [[CrossRef](#)]
81. Ge, H.; Ma, Z. Microwave preparation of triethylenetetramine modified graphene oxide/chitosan composite for adsorption of Cr(VI). *Carbohydr. Polym.* **2015**, *131*, 280–287. [[CrossRef](#)]
82. Kyzas, G.Z.; Sifaka, P.I.; Bikiaris, D.N.; Koukaras, E.N.; Froudakis, G.E. Alternative use of cross-linked polyallylamine (known as Sevelamer pharmaceutical compound) as biosorbent. *J. Colloid Interface Sci.* **2015**, *442*, 49–59. [[CrossRef](#)]
83. Li, L.; Fan, L.; Sun, M.; Qiu, H.; Li, X.; Duan, H.; Luo, C. Adsorbent for chromium removal based on graphene oxide functionalized with magnetic cyclodextrin–chitosan. *Colloids Surf. B Biointerfaces* **2013**, *107*, 76–83. [[CrossRef](#)] [[PubMed](#)]
84. Li, L.; Liu, F.; Duan, H.; Wang, X.; Li, J.; Wang, Y.; Luo, C. The preparation of novel adsorbent materials with efficient adsorption performance for both chromium and methylene blue. *Colloids Surf. B Biointerfaces* **2016**, *141*, 253–259. [[CrossRef](#)] [[PubMed](#)]
85. Guo, F.Y.; Liu, Y.G.; Wang, H.; Zeng, G.M.; Hu, X.J.; Zheng, B.H.; Li, T.T.; Tan, X.F.; Wang, S.F.; Zhang, M.M. Adsorption behavior of Cr(vi) from aqueous solution onto magnetic graphene oxide functionalized with 1,2-diaminocyclohexanetraacetic acid. *RSC Adv.* **2015**, *5*, 45384–45392. [[CrossRef](#)]
86. Hu, X.J.; Liu, Y.G.; Wang, H.; Chen, A.W.; Zeng, G.M.; Liu, S.M.; Guo, Y.M.; Hu, X.; Li, T.T.; Wang, Y.Q.; et al. Removal of Cu(II) ions from aqueous solution using sulfonated magnetic graphene oxide composite. *Sep. Purif. Technol.* **2013**, *108*, 189–195. [[CrossRef](#)]
87. Cui, L.; Wang, Y.; Gao, L.; Hu, L.; Yan, L.; Wei, Q.; Du, B. EDTA functionalized magnetic graphene oxide for removal of Pb(II), Hg(II) and Cu(II) in water treatment: Adsorption mechanism and separation property. *Chem. Eng. J.* **2015**, *281*, 1–10. [[CrossRef](#)]
88. Algothmi, W.M.; Bandaru, N.M.; Yu, Y.; Shapter, J.G.; Ellis, A.V. Alginate–graphene oxide hybrid gel beads: An efficient copper adsorbent material. *J. Colloid Interface Sci.* **2013**, *397*, 32–38. [[CrossRef](#)]
89. Chen, J.H.; Xing, H.T.; Sun, X.; Su, Z.B.; Huang, Y.H.; Weng, W.; Hu, S.R.; Guo, H.X.; Wu, W.B.; He, Y.S. Highly effective removal of Cu(II) by triethylenetetramine-magnetic reduced graphene oxide composite. *Appl. Surf. Sci.* **2015**, *356*, 355–363. [[CrossRef](#)]
90. Jiao, C.; Xiong, J.; Tao, J.; Xu, S.; Zhang, D.; Lin, H.; Chen, Y. Sodium alginate/graphene oxide aerogel with enhanced strength–toughness and its heavy metal adsorption study. *Int. J. Biol. Macromol.* **2016**, *83*, 133–141. [[CrossRef](#)]
91. Xing, H.T.; Chen, J.H.; Sun, X.; Huang, Y.H.; Su, Z.B.; Hu, S.R.; Weng, W.; Li, S.X.; Guo, H.X.; Wu, W.B.; et al. NH₂-rich polymer/graphene oxide use as a novel adsorbent for removal of Cu(II) from aqueous solution. *Chem. Eng. J.* **2015**, *263*, 280–289. [[CrossRef](#)]
92. Tan, M.; Liu, X.; Li, W.; Li, H. Enhancing sorption capacities for copper(II) and lead(II) under weakly acidic conditions by 1-tryptophan-functionalized graphene oxide. *J. Chem. Eng. Data* **2015**, *60*, 1469–1475. [[CrossRef](#)]
93. Chen, D.; Zhang, H.; Yang, K.; Wang, H. Functionalization of 4-aminothiophenol and 3-aminopropyltriethoxysilane with graphene oxide for potential dye and copper removal. *J. Hazard. Mater.* **2016**, *310*, 179–187. [[CrossRef](#)] [[PubMed](#)]
94. Carpio, I.E.M.; Mangadlao, J.D.; Nguyen, H.N.; Advincula, R.C.; Rodrigues, D.F. Graphene oxide functionalized with ethylenediamine triacetic acid for heavy metal adsorption and anti-microbial applications. *Carbon* **2014**, *77*, 289–301. [[CrossRef](#)]
95. Chandra, V.; Kim, K.S. Highly selective adsorption of Hg²⁺ by a polypyrrole–reduced graphene oxide composite. *Chem. Commun.* **2011**, *47*, 3942–3944. [[CrossRef](#)] [[PubMed](#)]
96. Zhang, Y.; Yan, T.; Yan, L.; Guo, X.; Cui, L.; Wei, Q.; Du, B. Preparation of novel cobalt ferrite/chitosan grafted with graphene composite as effective adsorbents for mercury ions. *J. Mol. Liq.* **2014**, *198*, 381–387. [[CrossRef](#)]
97. Madarang, C.J.; Kim, H.Y.; Gao, G.; Wang, N.; Zhu, J.; Feng, H.; Gorrington, M.; Kasner, M.L.; Hou, S. Adsorption behavior of EDTA-graphene oxide for Pb (II) removal. *ACS Appl. Mater. Interfaces* **2012**, *4*, 1186–1193. [[CrossRef](#)]
98. Zhang, N.; Qiu, H.; Si, Y.; Wang, W.; Gao, J. Fabrication of highly porous biodegradable monoliths strengthened by graphene oxide and their adsorption of metal ions. *Carbon* **2011**, *49*, 827–837. [[CrossRef](#)]

99. Yang, Y.; Xie, Y.; Pang, L.; Li, M.; Song, X.; Wen, J.; Zhao, H. Preparation of reduced graphene oxide/poly(acrylamide) nanocomposite and its adsorption of Pb(II) and methylene blue. *Langmuir* **2013**, *29*, 10727–10736. [[CrossRef](#)]
100. He, Y.Q.; Zhang, N.N.; Wang, X.D. Adsorption of graphene oxide/chitosan porous materials for metal ions. *Chin. Chem. Lett.* **2011**, *22*, 859–862. [[CrossRef](#)]
101. Musico, Y.L.F.; Santos, C.M.; Dalida, M.L.P.; Rodrigues, D.F. Improved removal of lead(II) from water using a polymer-based graphene oxide nanocomposite. *J. Mater. Chem. A* **2013**, *1*, 3789–3796. [[CrossRef](#)]
102. Luo, S.; Xu, X.; Zhou, G.; Liu, C.; Tang, Y.; Liu, Y. Amino siloxane oligomer-linked graphene oxide as an efficient adsorbent for removal of Pb(II) from wastewater. *J. Hazard. Mater.* **2014**, *274*, 145–155. [[CrossRef](#)]
103. Xu, Z.; Zhang, Y.; Qian, X.; Shi, J.; Chen, L.; Li, B.; Niu, J.; Liu, L. One step synthesis of polyacrylamide functionalized graphene and its application in Pb(II) removal. *Appl. Surf. Sci.* **2014**, *316*, 308–314. [[CrossRef](#)]
104. Yang, J.; Wu, J.X.; Lü, Q.F.; Lin, T.T. Facile preparation of lignosulfonate-graphene oxide-polyaniline ternary nanocomposite as an effective adsorbent for Pb(II) ions. *ACS Sustain. Chem. Eng.* **2014**, *2*, 1203–1211. [[CrossRef](#)]
105. Yang, L.; Li, Z.; Nie, G.; Zhang, Z.; Lu, X.; Wang, C. Fabrication of poly(o-phenylenediamine)/reduced graphene oxide composite nanosheets via microwave heating and their effective adsorption of lead ions. *Appl. Surf. Sci.* **2014**, *307*, 601–607. [[CrossRef](#)]
106. Zou, X.; Yin, Y.; Zhao, Y.; Chen, D.; Dong, S. Synthesis of ferrihydrite/l-cysteine magnetic microspheres and their adsorption capacity for Pb(II) ions. *Mater. Lett.* **2015**, *150*, 59–61. [[CrossRef](#)]
107. Liu, Y.; Xu, L.; Liu, J.; Liu, X.; Chen, C.; Li, G.; Meng, Y. Graphene oxides cross-linked with hyperbranched polyethylenimines: Preparation, characterization and their potential as recyclable and highly efficient adsorption materials for lead(II) ions. *Chem. Eng. J.* **2016**, *285*, 698–708. [[CrossRef](#)]
108. Hu, L.; Yang, Z.; Cui, L.; Li, Y.; Ngo, H.H.; Wang, Y.; Wei, Q.; Ma, H.; Yan, L.; Du, B. Fabrication of hyperbranched polyamine functionalized graphene for high-efficiency removal of Pb(II) and methylene blue. *Chem. Eng. J.* **2016**, *287*, 545–556. [[CrossRef](#)]
109. Qi, H.; Liu, H.; Gao, Y. Removal of Sr(II) from aqueous solutions using polyacrylamide modified graphene oxide composites. *J. Mol. Liq.* **2015**, *208*, 394–401. [[CrossRef](#)]
110. Chen, S.; Hong, J.; Yang, H.; Yang, J. Adsorption of uranium (VI) from aqueous solution using a novel graphene oxide-activated carbon felt composite. *J. Environ. Radioact.* **2013**, *126*, 253–258. [[CrossRef](#)]
111. Chen, L.; Zhao, D.; Chen, S.; Wang, X.; Chen, C. One-step fabrication of amino functionalized magnetic graphene oxide composite for uranium(VI) removal. *J. Colloid. Interface Sci.* **2016**, *472*, 99–107. [[CrossRef](#)]
112. Yap, P.L.; Nine, M.J.; Hassan, K.; Tung, T.T.; Tran, D.N.H.; Losic, D. Graphene-Based Sorbents for Multipollutants Removal in Water: A Review of Recent Progress. *Adv. Funct. Mater.* **2021**, *31*, 2007356. [[CrossRef](#)]
113. Sum, J.Y.; Ahmad, A.L.; Ooi, B.S. Selective separation of heavy metal ions using amine-rich polyamide TFC membrane. *J. Ind. Eng. Chem.* **2019**, *76*, 277–287. [[CrossRef](#)]
114. Jin, T.; Easton, C.D.; Yin, H.; de Vries, M.; Hao, X. Triethylenetetramine/hydroxyethyl cellulose-functionalized graphene oxide monoliths for the removal of copper and arsenate ions. *Sci. Technol. Adv. Mater.* **2018**, *19*, 381–395. [[CrossRef](#)]
115. Adel, M.; Ahmed, M.A.; Elabadi, M.A.; Mohamed, A.A. Removal of heavy metals and dyes from wastewater using graphene oxide-based nanomaterials: A critical review. *Environ. Nanotechnol. Monit. Manag.* **2022**, *18*, 100719. [[CrossRef](#)]
116. Ahmad, H.; Umar, K.; Ali, S.G.; Singh, P.; Islam, S.S.; Khan, H.M. Preconcentration and speciation of arsenic by using a graphene oxide nanoconstruct functionalized with a hyperbranched polyethyleneimine. *Microchim. Acta* **2018**, *185*, 290. [[CrossRef](#)] [[PubMed](#)]
117. Kislenco, V.N.; Oliynyk, L.P. Complex formation of polyethyleneimine with copper(II), nickel(II), and cobalt(II) ions. *J. Polym. Sci. A Polym. Chem.* **2002**, *40*, 914–922. [[CrossRef](#)]
118. Bafroee, A.A.T.; Moniri, E.; Panahi, H.A.; Miralinaghi, M.; Hasani, A.H. Ethylenediamine functionalized magnetic graphene oxide (Fe₃O₄@GO-EDA) as an efficient adsorbent in Arsenic(III) decontamination from aqueous solution. *Res. Chem. Intermed.* **2021**, *47*, 1397–1428. [[CrossRef](#)]
119. Gerçel, Ö.; Gerçel, H.F. Adsorption of lead(II) ions from aqueous solutions by activated carbon prepared from biomass plant material of *Euphorbia rigida*. *Chem. Eng. J.* **2007**, *132*, 289–297. [[CrossRef](#)]
120. Mahadevi, A.S.; Sastry, G.N. Cation- π interaction: Its role and relevance in chemistry, biology, and material science. *Chem. Rev.* **2013**, *113*, 2100–2138. [[CrossRef](#)]
121. Ren, Y.; Yan, N.; Feng, J.; Ma, J.; Wen, Q.; Li, N.; Dong, Q. Adsorption mechanism of copper and lead ions onto graphene nanosheet/ δ -MnO₂. *Mater. Chem. Phys.* **2012**, *136*, 538–544. [[CrossRef](#)]
122. Choi, J.S.; Lingamdinne, L.P.; Yang, J.K.; Chang, Y.Y.; Koduru, J.R. Fabrication of chitosan/graphene oxide-gadolinium nanorods as a novel nanocomposite for arsenic removal from aqueous solutions. *J. Mol. Liq.* **2020**, *320*, 114410. [[CrossRef](#)]
123. Lingamdinne, L.P.; Lee, S.; Choi, J.S.; Lebaka, V.R.; Durbaka, V.R.P.; Koduru, J.R. Potential of the magnetic hollow sphere nanocomposite (graphene oxide-gadolinium oxide) for arsenic removal from real field water and antimicrobial applications. *J. Hazard. Mater.* **2021**, *402*, 123882. [[CrossRef](#)] [[PubMed](#)]
124. Joya-Cárdenas, D.R.; Rodríguez-Caicedo, J.P.; Gallegos-Muñoz, A.; Zanoor, G.A.; Caycedo-García, M.S.; Damian-Ascencio, C.E.; Saldaña-Robles, A. Graphene-Based Adsorbents for Arsenic, Fluoride, and Chromium Adsorption: Synthesis Methods Review. *Nanomaterials* **2022**, *12*, 3942. [[CrossRef](#)] [[PubMed](#)]
125. Lou, M.; Huang, S.; Zhu, X.; Chen, J.; Fang, X.; Li, F. Dual-polymers inserted graphene oxide membranes with enhanced anti-wetting and anti-scaling performance for membrane distillation. *J. Memb. Sci.* **2024**, *697*, 122494. [[CrossRef](#)]

126. Kong, Q.; Shi, X.; Ma, W.; Zhang, F.; Yu, T.; Zhao, F.; Zhao, D.; Wei, C. Strategies to improve the adsorption properties of graphene-based adsorbent towards heavy metal ions and their compound pollutants: A review. *J. Hazard. Mater.* **2021**, *415*, 125690. [[CrossRef](#)]
127. Gholami, F.; Ghanizadeh, G.; Zinatizadeh, A.A.; Zinadini, S.; Masoumbeigi, H. Arsenic and total dissolved solids removal using antibacterial/antifouling nanofiltration membranes modified by functionalized graphene oxide and copper ferrodioxide. *Water Environ. Res.* **2023**, *95*, e10902. [[CrossRef](#)]
128. Janwery, D.; Memon, F.H.; Memon, A.A.; Iqbal, M.; Memon, F.N.; Ali, W.; Choi, K.H.; Thebo, K.H. Lamellar Graphene Oxide-Based Composite Membranes for Efficient Separation of Heavy Metal Ions and Desalination of Water. *ACS Omega* **2023**, *8*, 7648–7656. [[CrossRef](#)]
129. Koli, M.; Ranjan, R.; Singh, S.P. Functionalized graphene-based ultrafiltration and thin-film composite nanofiltration membranes for arsenic, chromium, and fluoride removal from simulated groundwater: Mechanism and effect of pH. *Process Saf. Environ. Prot.* **2023**, *179*, 603–617. [[CrossRef](#)]
130. Zhang, P.; Gong, J.L.; Zeng, G.M.; Deng, C.H.; Yang, H.C.; Liu, H.Y.; Huan, S.Y. Cross-linking to prepare composite graphene oxide-framework membranes with high-flux for dyes and heavy metal ions removal. *Chem. Eng. J.* **2017**, *322*, 657–666. [[CrossRef](#)]
131. Mahmoudian, M.; Kochameshki, M.G.; Hosseinzadeh, M. Modification of graphene oxide by ATRP: A pH-responsive additive in membrane for separation of salts, dyes and heavy metals. *J. Environ. Chem. Eng.* **2018**, *6*, 3122–3134. [[CrossRef](#)]
132. Zhang, Y.; Zhang, S.; Chung, T.S. Nanometric Graphene Oxide Framework Membranes with Enhanced Heavy Metal Removal via Nanofiltration. *Environ. Sci. Technol.* **2015**, *49*, 10235–10242. [[CrossRef](#)] [[PubMed](#)]
133. Zhao, S.; Zhu, H.; Wang, H.; Rassu, P.; Wang, Z.; Song, P.; Rao, D. Free-standing graphene oxide membrane with tunable channels for efficient water pollution control. *J. Hazard. Mater.* **2019**, *366*, 659–668. [[CrossRef](#)] [[PubMed](#)]
134. Bandedhali, S.; Moghadassi, A.; Parvizian, F.; Zhang, Y.; Hosseini, S.M.; Shen, J. New mixed matrix PEI nanofiltration membrane decorated by glycidyl-POSS functionalized graphene oxide nanoplates with enhanced separation and antifouling behaviour: Heavy metal ions removal. *Sep. Purif. Technol.* **2020**, *242*, 116745. [[CrossRef](#)]
135. Lin, H.; Li, Y.; Zhu, J. Cross-linked GO membranes assembled with GO nanosheets of differently sized lateral dimensions for organic dye and chromium separation. *J. Memb. Sci.* **2020**, *598*, 117789. [[CrossRef](#)]
136. Abdi, G.; Alizadeh, A.; Zinadini, S.; Moradi, G. Removal of dye and heavy metal ion using a novel synthetic polyethersulfone nanofiltration membrane modified by magnetic graphene oxide/metformin hybrid. *J. Memb. Sci.* **2018**, *552*, 326–335. [[CrossRef](#)]
137. Zhang, Y.; Su, K.; Li, Z. Graphene oxide composite membranes cross-linked with urea for enhanced desalting properties. *J. Memb. Sci.* **2018**, *563*, 718–725. [[CrossRef](#)]
138. Ghaffar, A.; Zhang, L.; Zhu, X.; Chen, B. Scalable graphene oxide membranes with tunable water channels and stability for ion rejection. *Environ. Sci. Nano* **2019**, *6*, 904–915. [[CrossRef](#)]
139. Zhang, N.; Qi, W.; Huang, L.; Jiang, E.; Bao, J.; Zhang, X.; An, B.; He, G. Review on structural control and modification of graphene oxide-based membranes in water treatment: From separation performance to robust operation. *Chin. J. Chem. Eng.* **2019**, *27*, 1348–1360. [[CrossRef](#)]
140. Sun, J.; Hu, C.; Liu, Z.; Liu, H.; Qu, J. Surface charge and hydrophilicity improvement of graphene membranes via modification of pore surface oxygen-containing groups to enhance permeability and selectivity. *Carbon* **2019**, *145*, 140–148. [[CrossRef](#)]
141. An, Y.C.; Gao, X.X.; Jiang, W.L.; Han, J.L.; Ye, Y.; Chen, T.M.; Ren, R.Y.; Zhang, J.H.; Liang, B.; Li, Z.L.; et al. A critical review on graphene oxide membrane for industrial wastewater treatment. *Environ. Res.* **2023**, *223*, 115409. [[CrossRef](#)]
142. Cha-Umpong, W.; Hosseini, E.; Razmjou, A.; Zakertabrizi, M.; Korayem, A.H.; Chen, V. New molecular understanding of hydrated ion trapping mechanism during thermally-driven desalination by pervaporation using GO membrane. *J. Memb. Sci.* **2020**, *598*, 117687. [[CrossRef](#)]
143. Wang, P.; Jia, Y.X.; Yan, R.; Wang, M. Graphene oxide proton permselective membrane for electrodialysis-based waste acid reclamation: Simulation and validation. *J. Memb. Sci.* **2021**, *640*, 119853. [[CrossRef](#)]
144. Andreeva, D.V.; Trushin, M.; Nikitina, A.; Costa, M.C.F.; Cherepanov, P.V.; Holwill, M.; Chen, S.; Yang, K.; Chee, S.W.; Mirsaidov, U.; et al. Two-dimensional adaptive membranes with programmable water and ionic channels. *Nat. Nanotechnol.* **2021**, *16*, 174–180. [[CrossRef](#)]
145. Galama, A.H.; Post, J.W.; Stuart, M.A.C.; Biesheuvel, P.M. Validity of the Boltzmann equation to describe Donnan equilibrium at the membrane-solution interface. *J. Memb. Sci.* **2013**, *442*, 131–139. [[CrossRef](#)]
146. Verma, B.; Balomajumder, C.; Sabapathy, M.; Gumfekar, S.P. Pressure-driven membrane process: A review of advanced technique for heavy metals remediation. *Processes* **2021**, *9*, 752. [[CrossRef](#)]
147. Su, P.; Wang, F.; Li, Z.; Tang, C.Y.; Li, W. Graphene oxide membranes: Controlling their transport pathways. *J. Mater. Chem. A Mater.* **2020**, *8*, 15319–15340. [[CrossRef](#)]
148. Yang, T.; Lin, H.; Loh, K.P.; Jia, B. Fundamental Transport Mechanisms and Advancements of Graphene Oxide Membranes for Molecular Separation. *Chem. Mater.* **2019**, *31*, 1829–1846. [[CrossRef](#)]
149. Saavedra, A.; Valdés, H.; Velásquez, J.; Hernández, S. Comparative Analysis of Donnan Steric Partitioning Pore Model and Dielectric Exclusion Applied to the Fractionation of Aqueous Saline Solutions through Nanofiltration. *ChemEngineering* **2024**, *8*, 39. [[CrossRef](#)]
150. Quintano, V.; Kovtun, A.; Biscarini, F.; Liscio, F.; Liscio, A.; Palermo, V. Long-range selective transport of anions and cations in graphene oxide membranes, causing selective crystallization on the macroscale. *Nanoscale Adv.* **2021**, *3*, 353–358. [[CrossRef](#)]

151. Zhang, W.; Li, J.S.; Chen, S.X.; Huang, K.; Luo, L.J.; Tong, K.W.; Guo, J.H.; Li, S.C.; Zhang, R.; Dai, Z.J. Effect of layer charge density and cation concentration on sorption behaviors of heavy metal ions in the interlayer and nanopore of montmorillonite: A molecular dynamics simulation. *Colloids Surf. A Physicochem. Eng. Asp.* **2023**, *657*, 130553. [[CrossRef](#)]
152. Niu, Y.; Yu, W.; Yang, S.; Wan, Q. Understanding the relationship between pore size, surface charge density, and Cu²⁺ adsorption in mesoporous silica. *Sci. Rep.* **2024**, *14*, 13521. [[CrossRef](#)]
153. Kalaitzidou, K.; Nikolettopoulos, A.A.; Tsiftsakis, N.; Pinakidou, F.; Mitrakas, M. Adsorption of Se(IV) and Se(VI) species by iron oxy-hydroxides: Effect of positive surface charge density. *Sci. Total Environ.* **2019**, *687*, 1197–1206. [[CrossRef](#)]
154. Osorio, S.C.; Biesheuvel, P.M.; Dykstra, J.E.; Virga, E. Nanofiltration of complex mixtures: The effect of the adsorption of divalent ions on membrane retention. *Desalination* **2022**, *527*, 115552. [[CrossRef](#)]
155. Li, K.; Tao, Y.; Li, Z.; Sha, J.; Chen, Y. Selective ion-permeation through strained and charged graphene membranes. *Nanotechnology* **2017**, *29*, 035402. [[CrossRef](#)] [[PubMed](#)]
156. Dutta, M.; Bairoju, S.; De, S. Simplistic determination of the membrane pore charge density in presence of mixture of electrolytes. *J. Memb. Sci.* **2023**, *675*, 121577. [[CrossRef](#)]
157. Hagemeyer, G.; Gimbel, R. Modelling the rejection of nanofiltration membranes using zeta potential measurements. *Sep. Purif. Technol.* **1999**, *15*, 19–30. [[CrossRef](#)]
158. Velusamy, S.; Roy, A.; Sundaram, S.; Mallick, T.K. A Review on Heavy Metal Ions and Containing Dyes Removal Through Graphene Oxide-Based Adsorption Strategies for Textile Wastewater Treatment. *Chem. Rec.* **2021**, *21*, 1570–1610. [[CrossRef](#)]
159. Li, X.; Zhou, H.; Wu, W.; Wei, S.; Xu, Y.; Kuang, Y. Studies of heavy metal ion adsorption on Chitosan/Sulfydryl-functionalized graphene oxide composites. *J. Colloid. Interface Sci.* **2015**, *448*, 389–397. [[CrossRef](#)]
160. Sahraei, R.; Hemmati, K.; Ghaemy, M. Adsorptive removal of toxic metals and cationic dyes by magnetic adsorbent based on functionalized graphene oxide from water. *RSC Adv.* **2016**, *6*, 72487–72499. [[CrossRef](#)]
161. Zhang, Z.; Gao, T.; Si, S.; Liu, Q.; Wu, Y.; Zhou, G. One-pot preparation of P(TA-TEPA)-PAM-RGO ternary composite for high efficient Cr(VI) removal from aqueous solution. *Chem. Eng. J.* **2018**, *343*, 207–216. [[CrossRef](#)]
162. Qalyoubi, L.; Al-Othman, A.; Al-Asheh, S. Recent progress and challenges on adsorptive membranes for the removal of pollutants from wastewater. *Part. I Fundam. Classif. Membr. Case Stud. Chem. Environ. Eng.* **2021**, *3*, 100086. [[CrossRef](#)]

Disclaimer/Publisher’s Note: The statements, opinions and data contained in all publications are solely those of the individual author(s) and contributor(s) and not of MDPI and/or the editor(s). MDPI and/or the editor(s) disclaim responsibility for any injury to people or property resulting from any ideas, methods, instructions or products referred to in the content.